Selected Topics in Nuclear and Atomic Physics 2022

29 September 2022 - Fiera di Primiero (TN)

Shape and deformation in nuclei: quantum phase transition in Zr isotopes studied via lifetime measurements

Giorgia Pasqualato

IJCLab
Irène Joliot-Curie
Laboratoire de Physique des 2 Infinis

G. Pasqualato[1], A. Görgen[2], J.S. Heines[2], J. Ljungvall[1], V. Modamio[2], L.G. Pedersen[2], and W. Korten[3]

[1] *IJCLab, IN2P3/CNRS, Université Paris-Saclay, Orsay, France.*
[2] *Department of Physics, University of Oslo, Norway.*
[3] *CEA Paris-Saclay, DRF/IRFU/DPhN, Gif-sur-Yvette, France.*

- INTRODUCTION :
  - Deformation and shapes in nuclei.
  - How can we study them from experiments?
  - Quantum phase transition in Zr isotopes.

- EXPERIMENT :
  - The experimental setup AGATA+VAMOS+plunger.
  - Lifetime measurements with the RDDS technique.

- ANALYSIS :
  - Lifetime results for 98-104Zr.
  - Comparison with theoretical predictions: MCSM, IBM-CM and SCCM-HFB.

- INTRODUCTION :
  - Deformation and shapes in nuclei.
  - How can we study them from experiments?
  - Quantum phase transition in Zr isotopes.

- EXPERIMENT :
  - The experimental setup AGATA+VAMOS+plunger.
  - Lifetime measurements with the RDDS technique.

- ANALYSIS :
  - Lifetime results for 98-104Zr.
  - Comparison with theoretical predictions: MCSM, IBM-CM and SCCM-HFB.

Why nuclear shapes ?

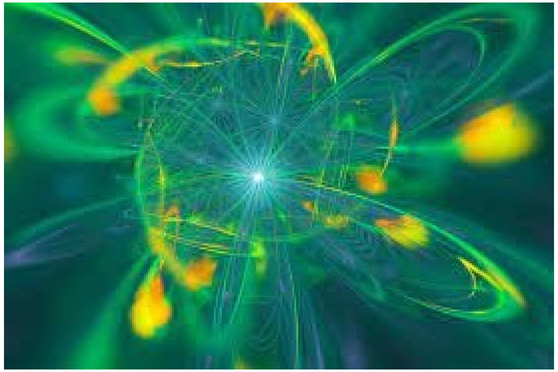

- The nucleus is a complex many-body quantum system.
- Need of a **simplification** to describe its behavior.

    - Where does nuclear shape come from ?

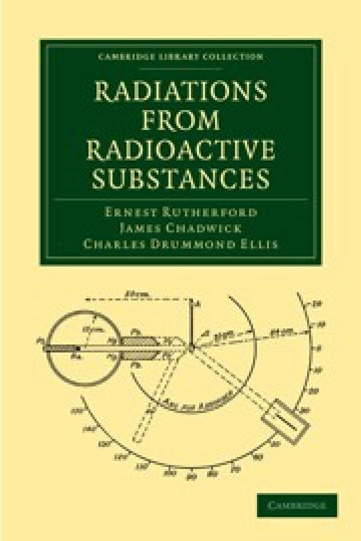

1911

In the famous scattering experiment Rutherford shows that the nucleus has a small but sizable spatial extension → (spherical) shape.

1935

Schüler and Schmidt : via atomic spectroscopy experiments, first clear indications of nuclear electric quadrupole moments (perturbation on the hyper-fine structure images in Eu reveals a deviation from the spherical symmetry.)

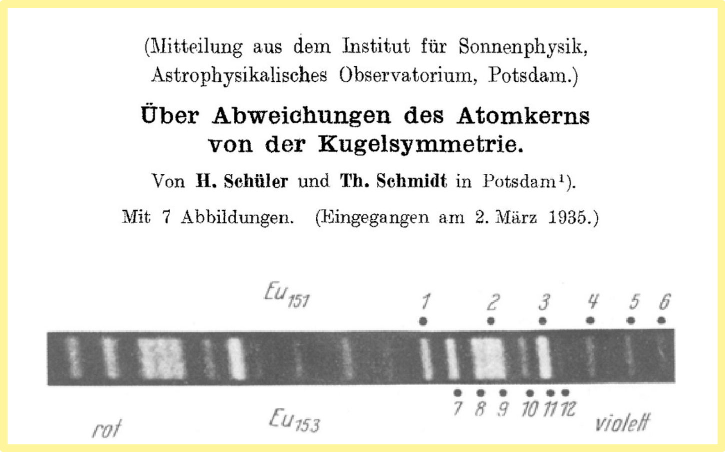

Why nuclear shapes ?

- Parametrization of the **radius** of the nuclear surface : $$R(\theta,\phi) = R_0 \left\{ 1 + \sum_{\lambda} \sum_{\mu=-\lambda}^{\lambda} a_{\lambda\mu} Y_{\lambda\mu}(\theta,\phi) \right\}$$

- Important basic shapes :
  - $\lambda = 2$ → quadrupole deformation
  - $\lambda = 3$ → octupole deformation

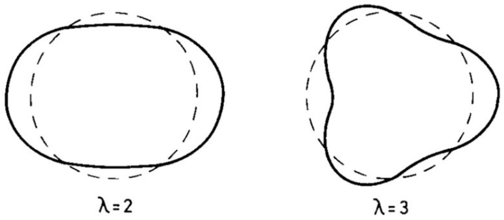

- In the principal axis frame $a_{2,1} = a_{2,-1} = 0$ and we define the Hill-Wheeler coordinates parameters β and γ for the mass surface :

  $a_{2,0} = \beta\cos(\gamma)$

  $a_{2,2} = \beta\sin(\gamma)/\sqrt{2}$ → rather simple description !

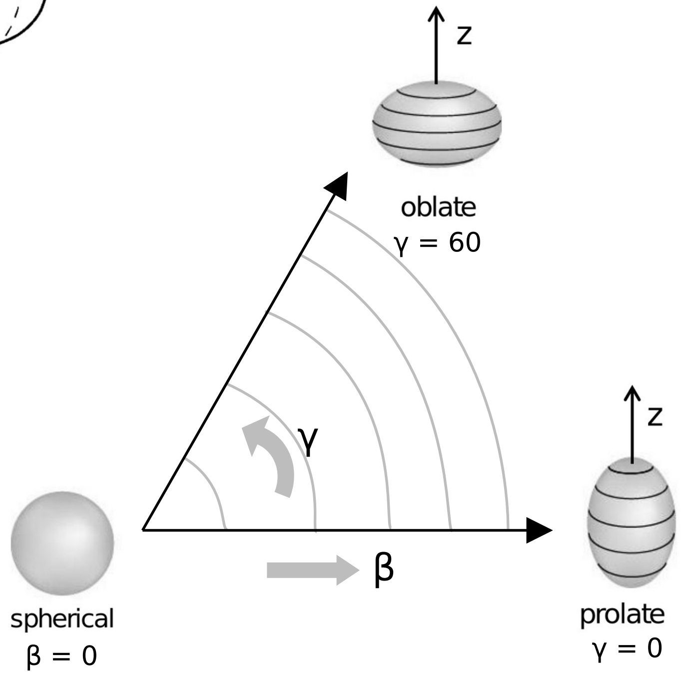

- ... but nuclear shape is not an observable.

Phenomenological manifestation of nuclear shapes

- The use of an intrinsic deformation explain many phenomenon :
  - energy of excited states (e.g. energy of the first 2^+, 3^- states, rotational bands)

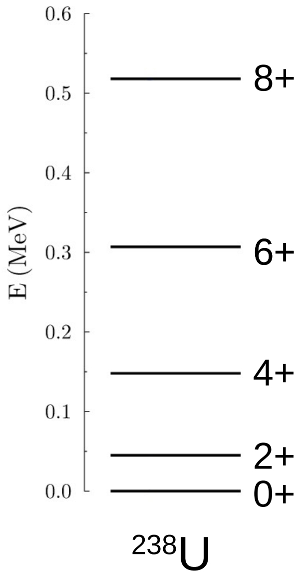

$$E(J) = \frac{J(J+1)}{2\mathcal{I}}$$

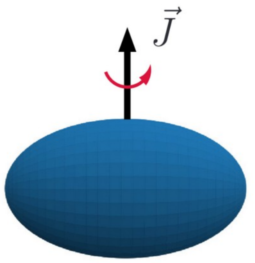

Semi-classical picture of a deformed nucleus rotating on its symmetry axis

(RIGID ROTOR = constant momentum of inertia $\mathcal{I}$)

Phenomenological manifestation of nuclear shapes

- The use of an intrinsic deformation explain many phenomenon :
  - energy of excited states
  - transition probabilities (e.g. B(E2;$2^+ \rightarrow 0^+$), B(E3; $3^- \rightarrow 0^+$))

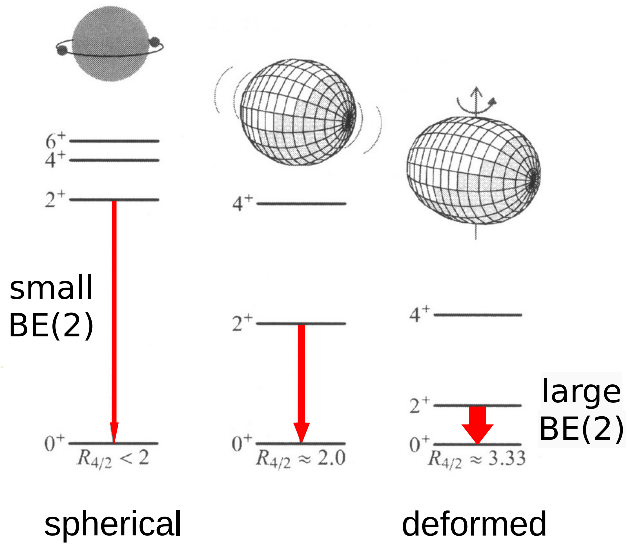

Phenomenological manifestation of nuclear shapes

- The use of an intrinsic deformation explain many phenomenon :
  - energy of excited states
  - transition probabilities
  - nuclear properties varying as a function of N, Z

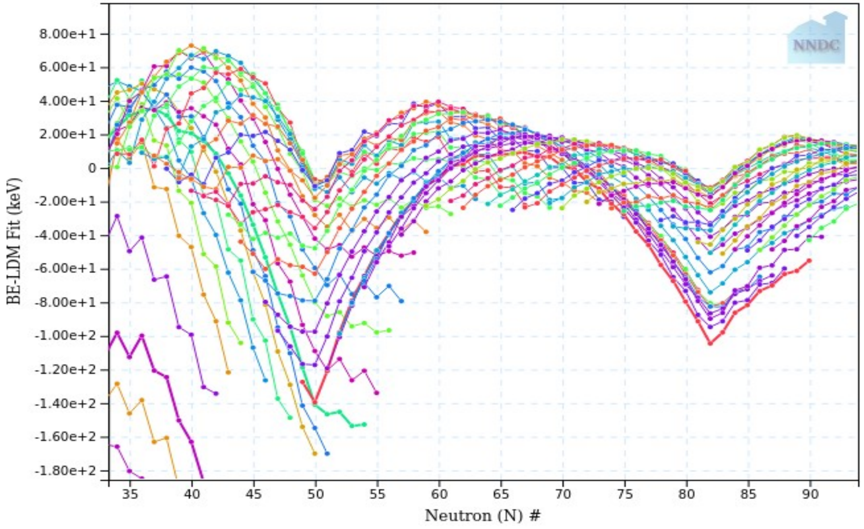

Phenomenological manifestation of nuclear shapes

- The use of an intrinsic deformation explain many phenomenon :
  - energy of excited states
  - transition probabilities
  - nuclear properties varying as a function of N, Z
  - high-energy heavy ion collision
  - …

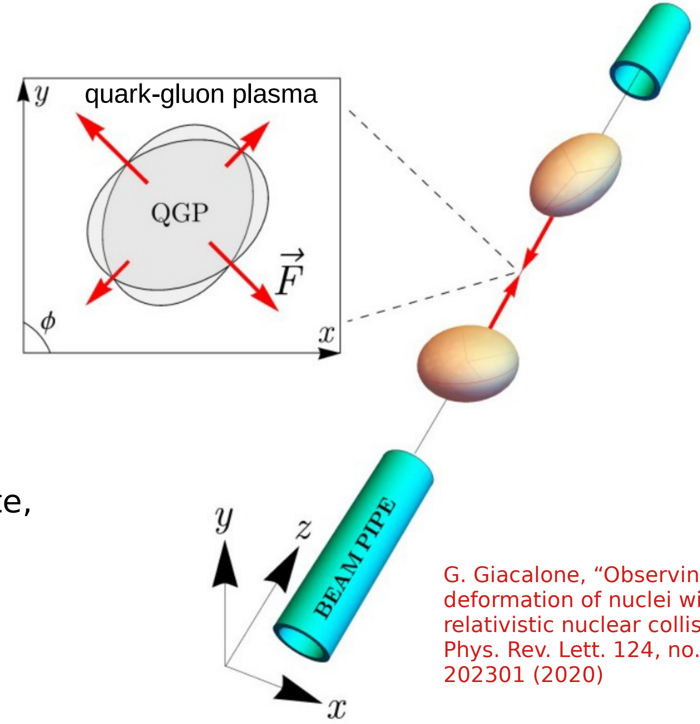

The nuclei, deformed in their ground state, are randomly oriented and influence the shape of their area of overlap.
A quark-gluon plasma (QGP) is formed in the this area.

G. Giacalone, “Observing the deformation of nuclei with relativistic nuclear collisions,” Phys. Rev. Lett. 124, no.20, 202301 (2020)

How can we "measure" nuclear shapes ?

- We are sensitive to the **charge distribution ρ(r)** via the electromagnetic interaction

Intrinsic electric quadrupole moments :

$$Q_0 = \int \rho(\vec{r})(3z^2 - r^2)dV$$

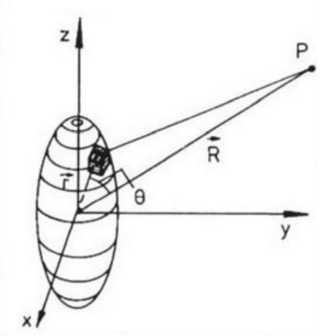

$Q_0 \neq 0$ → non-spherical charge distribution

How can we “measure” nuclear shapes ?

- We are sensitive to the **charge distribution ρ(r)** via the electromagnetic interaction

Intrinsic electric quadrupole moments :

$$Q_0 = \int \rho(\vec{r})(3z^2 - r^2)dV$$

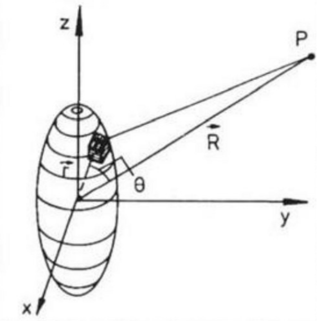

$Q_0 \neq 0$ → non-spherical charge distribution

And in the laboratory frame ?

- E2 transition probabilities (off-diagonal matrix elements)

$$B(E2; J_i \longrightarrow J_f) = \frac{1}{2J_i+1} |\langle J_f || M(E2) || J_i \rangle|^2$$

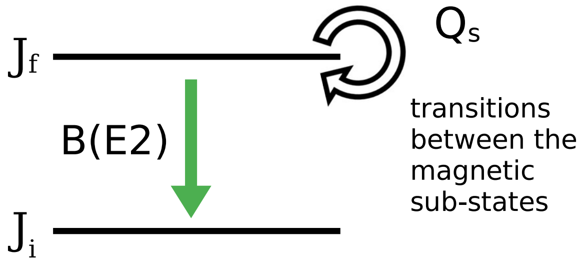

- Spectroscopic electric quadrupole moments (diagonal matrix elements)

$$Q_s(J) = \sqrt{\frac{16\pi}{5}} \frac{\langle J J 20 | J J \rangle}{\sqrt{2J+1}} \langle J || E2 || J \rangle$$

$Q_0 \neq Q_s$!

How can we “measure” nuclear shapes ?

Lifetime measurements

$$\frac{1}{\tau} \propto B(\pi\lambda; I_i \rightarrow I_f)$$

reduced transition probabilities

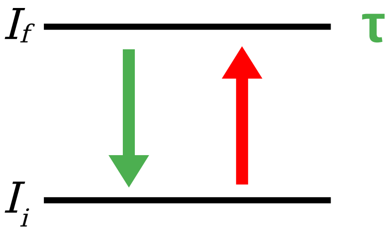

$$B(\sigma\lambda; I_i \rightarrow I_f)$$

This give us the shape?

NO

But …

Coulomb excitation

reduced transition probabilities

to first order: $\sigma_{\pi\lambda} \propto B(\pi\lambda; I_i \rightarrow I_f)$

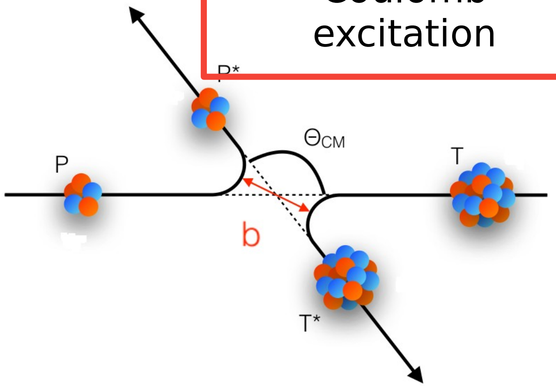

How can we "measure" nuclear shapes ?

Lifetime measurements

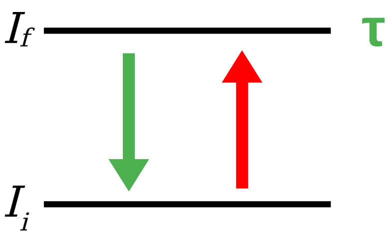

Coulomb excitation

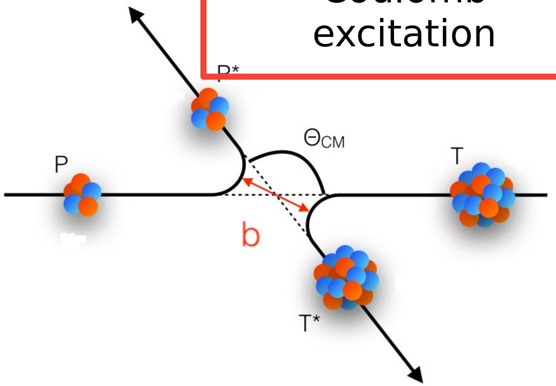

$$\frac{1}{\tau} \propto B(\pi\lambda; I_i \rightarrow I_f)$$

reduced transition probabilities

$$B(\sigma\lambda; I_i \rightarrow I_f)$$

reduced transition probabilities

to first order: $\sigma_{\pi\lambda} \propto B(\pi\lambda; I_i \rightarrow I_f)$

$$B(\sigma\lambda; I_i \rightarrow I_f) = \frac{1}{2I_i + 1} \left| \langle I_f \| \hat{O}(\sigma\lambda) \| I_i \rangle \right|^2$$

Matrix elements

Comparison with theoretical predictions

Quantitative test of nuclear models

Where do we encounter nuclear deformation ?

- The large amount of deformation is observed **far from magic lines**

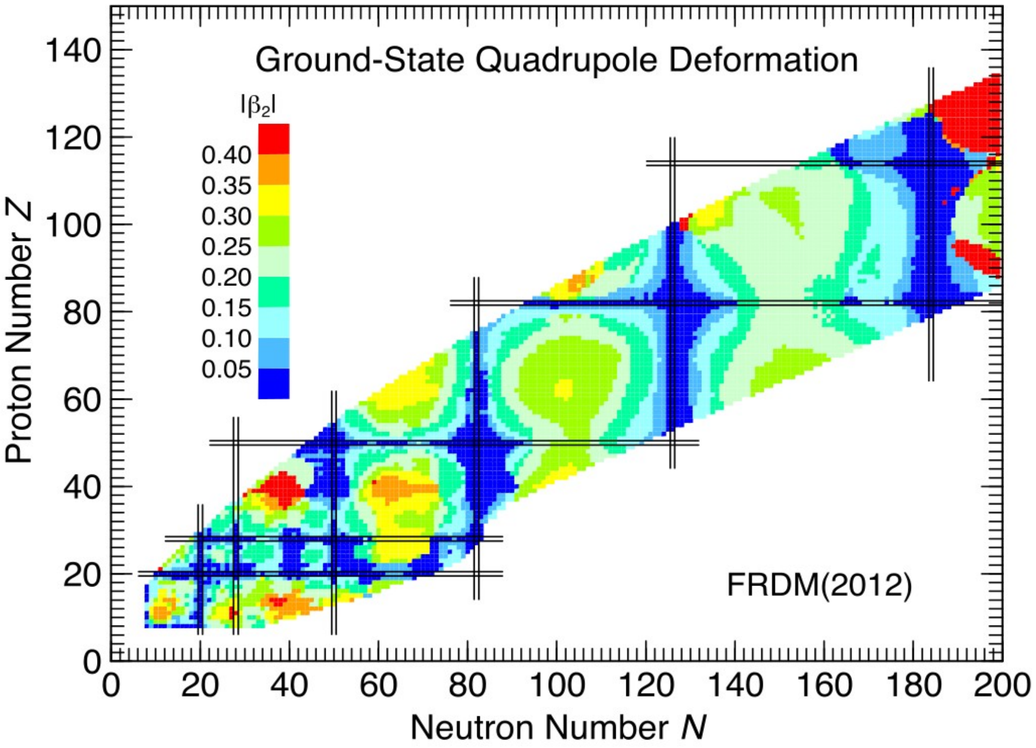

P. Möller, A.J. Sierk, T. Ichikawa, H. Sagawa, *Nuclear ground-state masses and deformations: FRDM(2012)*, Atomic Data and Nuclear Data Tables, 109–110, (2016),

- **Magic** numbers of Z and N over-stabilize the nucleus → spherical shape

Magic numbers are a clear evidence of the existence of an internal shell structure: a different picture with respect to a macroscopic view introduced by nuclear deformation

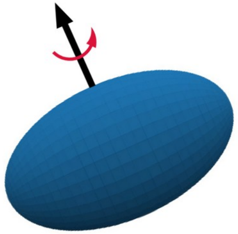

Macroscopic shape ⇔ microscopic structure

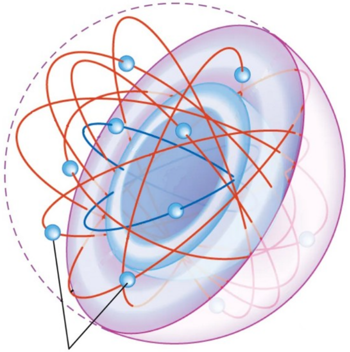

many nucleons outside a closed core → large collectivity = deformation

Shape coexistence

- **Shape coexistence** is a phenomenon where distinct shapes occur within the same nucleus and at a similar energy.

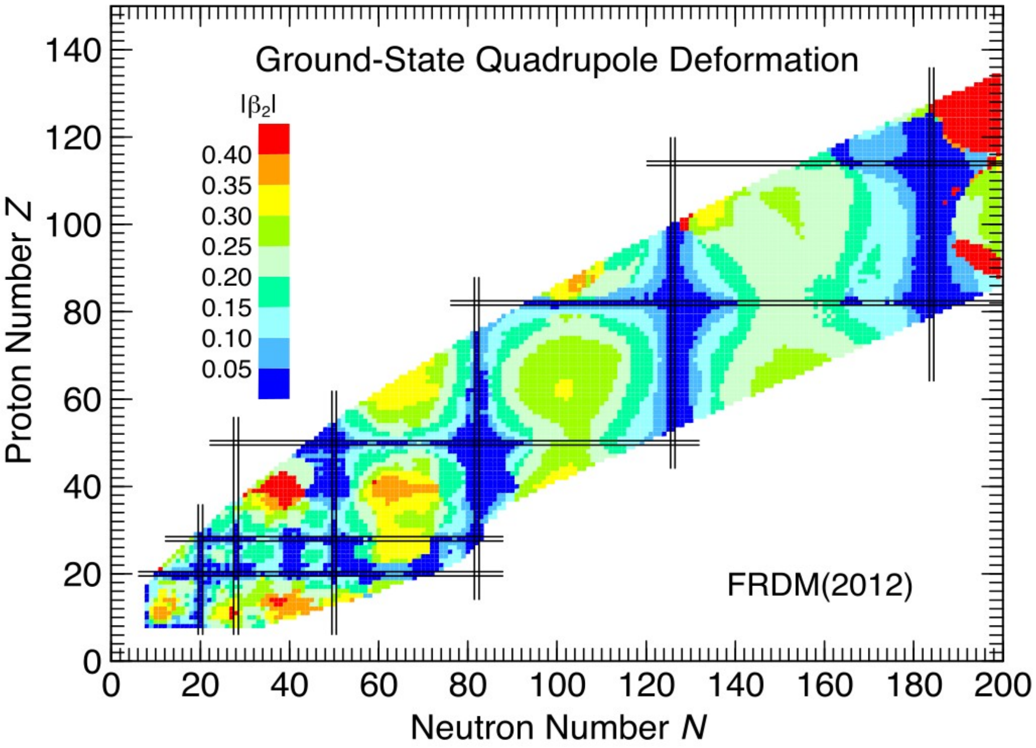

P. Möller, A.J. Sierk, T. Ichikawa, H. Sagawa, *Nuclear ground-state masses and deformations: FRDM(2012)*, Atomic Data and Nuclear Data Tables, 109–110, (2016),

^{186}Pb

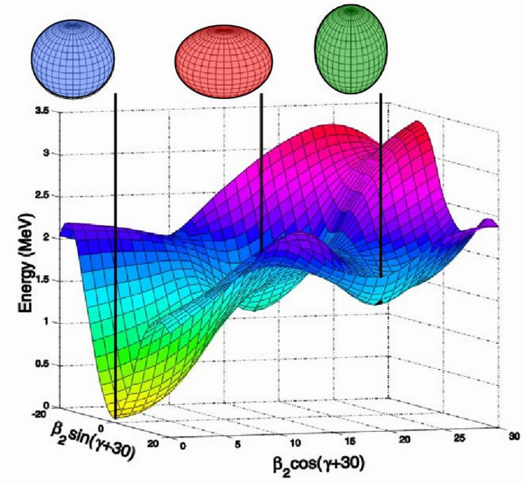

Often found in the boundaries of deformed regions in the nuclear chart as a consequence of the shape changing.

Shape coexistence

- **Shape coexistence** is a phenomenon where distinct shapes occur within the same nucleus and at a similar energy.

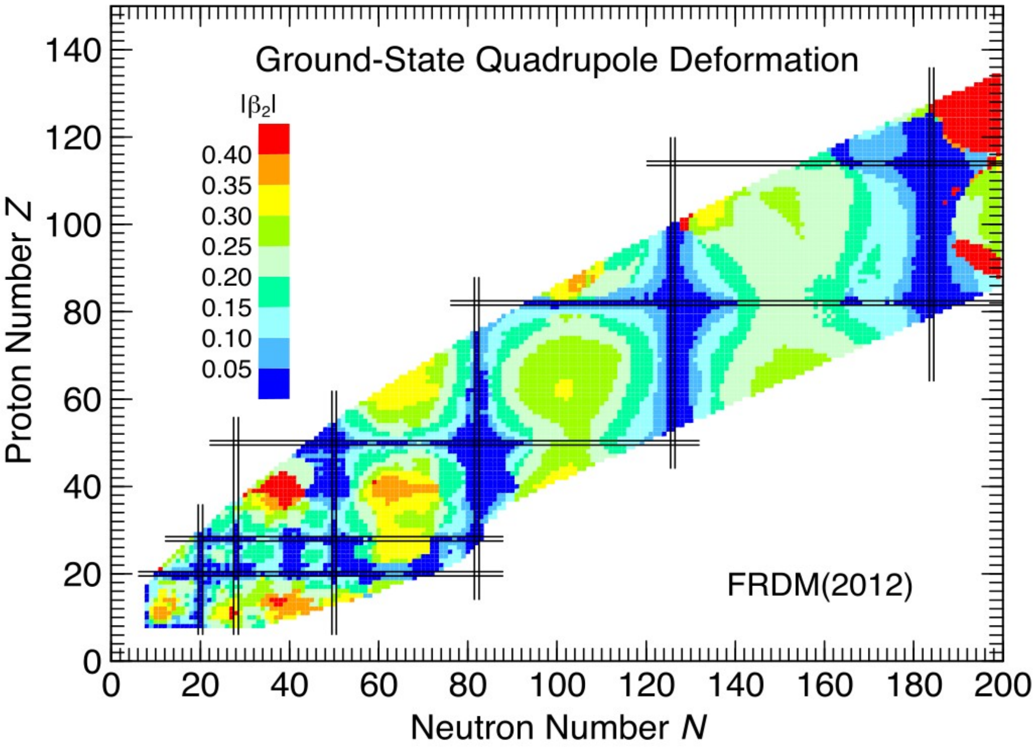

P. Möller, A.J. Sierk, T. Ichikawa, H. Sagawa, *Nuclear ground-state masses and deformations: FRDM(2012)*, Atomic Data and Nuclear Data Tables, 109–110, (2016),

^{186}**Pb**

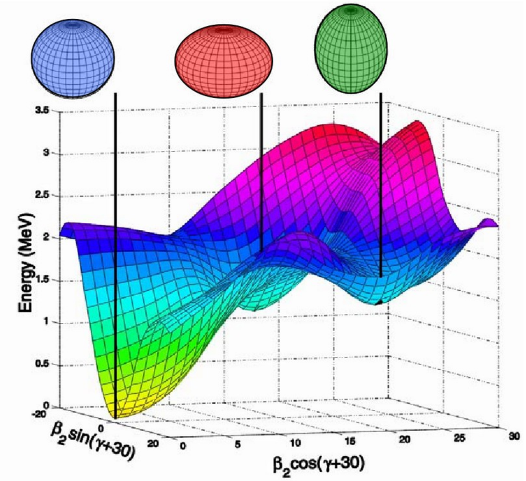

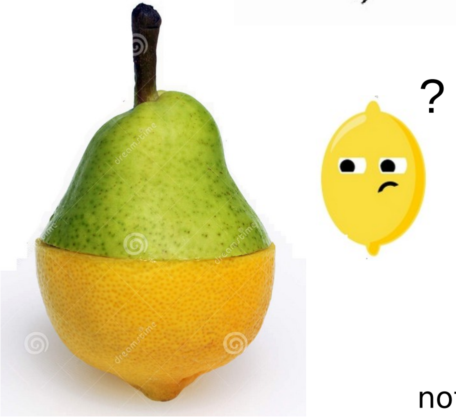

Coexistence of shapes?

not really

Shape coexistence

- **Shape coexistence** is a phenomenon where distinct shapes occur within the same nucleus and at a similar energy.

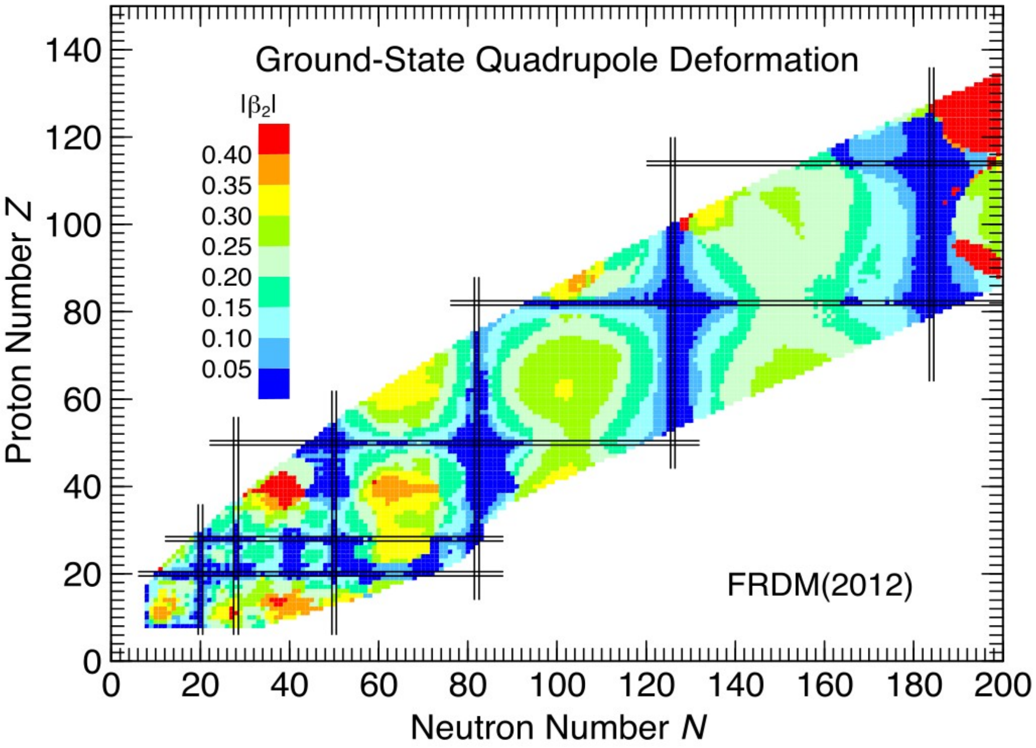

P. Möller, A.J. Sierk, T. Ichikawa, H. Sagawa, *Nuclear ground-state masses and deformations: FRDM(2012)*, Atomic Data and Nuclear Data Tables, 109–110, (2016),

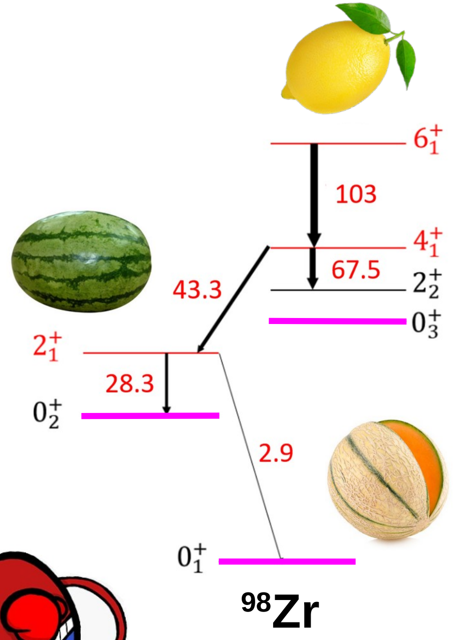

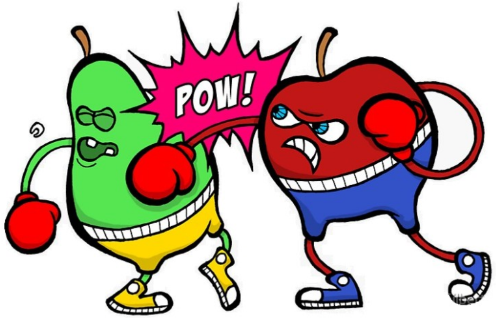

better to use this

Different configuration characterizing excited structure compete in energy to be the g.s. one

Shape evolution in neutron-rich nuclei around A=100

- Drastic onset of deformation in the the rare-earth region at N~90 or in Zr-Sr region around N=60.

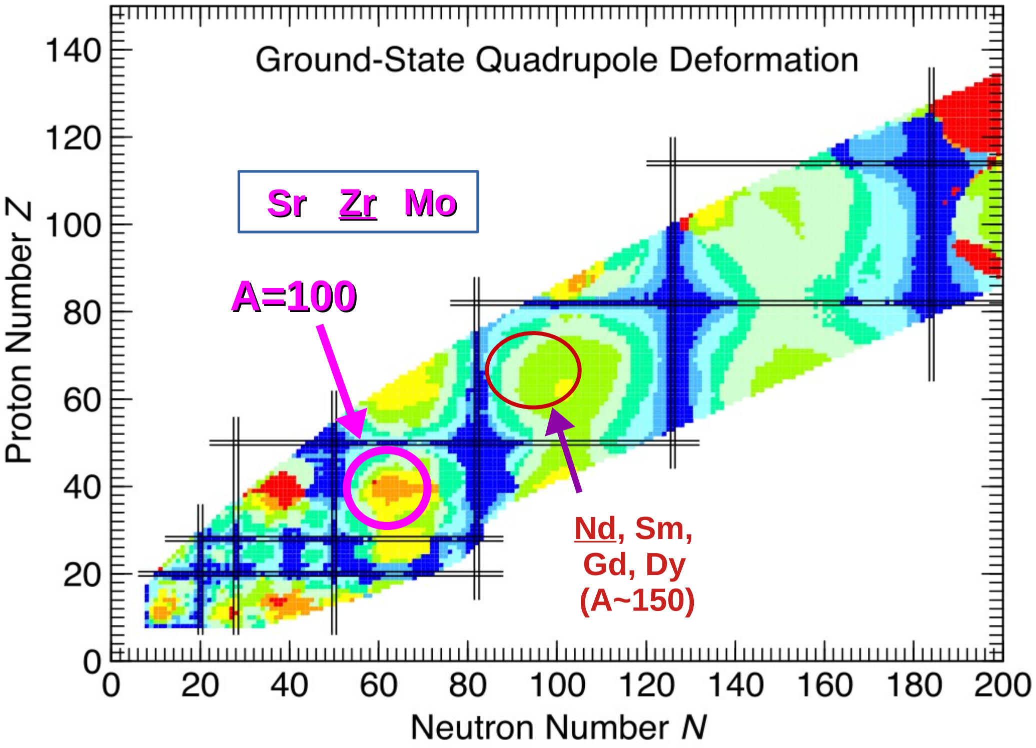

P. Möller, A.J. Sierk, T. Ichikawa, H. Sagawa, *Nuclear ground-state masses and deformations: FRDM(2012)*, Atomic Data and Nuclear Data Tables, 109–110, (2016),

Manifested via the rapid change of several nuclear observables as a function of N

e.g:

two-neutron separation energies,

energies E(J),

energy ratios $E(4_1^+)/E(2_1^+)$,

transition probabilities $B(E2:4_1^+ \to 2_1^+)$,

...

Shape evolution in neutron-rich nuclei around A=100

- Drastic onset of deformation in the the rare-earth region at N~90 or in Zr-Sr region around N=60.

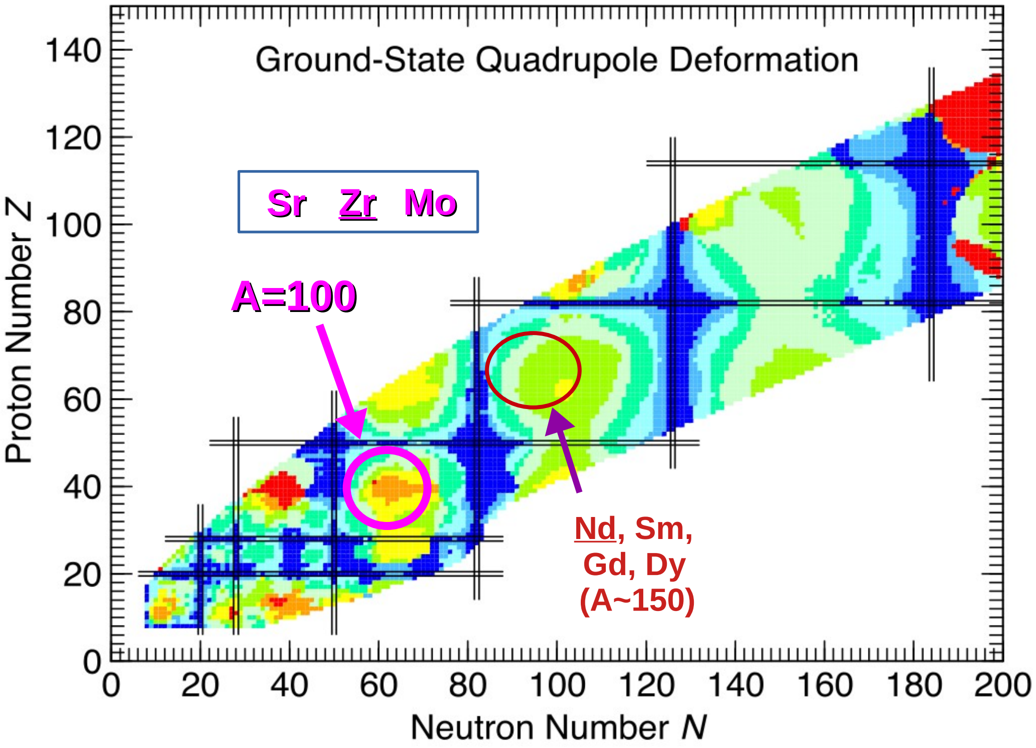

P. Möller, A.J. Sierk, T. Ichikawa, H. Sagawa, *Nuclear ground-state masses and deformations: FRDM(2012)*, Atomic Data and Nuclear Data Tables, 109–110, (2016),

Manifested via the rapid change of several nuclear observables as a function of N
e.g:
two-neutron separation energies,
energies E(J),
energy ratios $E(4_1^+)/E(2_1^+)$,
transition probabilities $B(E2:4_1^+ \rightarrow 2_1^+)$,
...

The term **quantum phase transition** (QPT) is used to describe this phenomenon, due to the similarities with the thermodynamic phase transitions.

P. Cejnar, J. Jolie and R.F. Casten, Rev. Mod. Phys. 82, 2155 (2010).

Shape evolution in neutron-rich nuclei around A=100

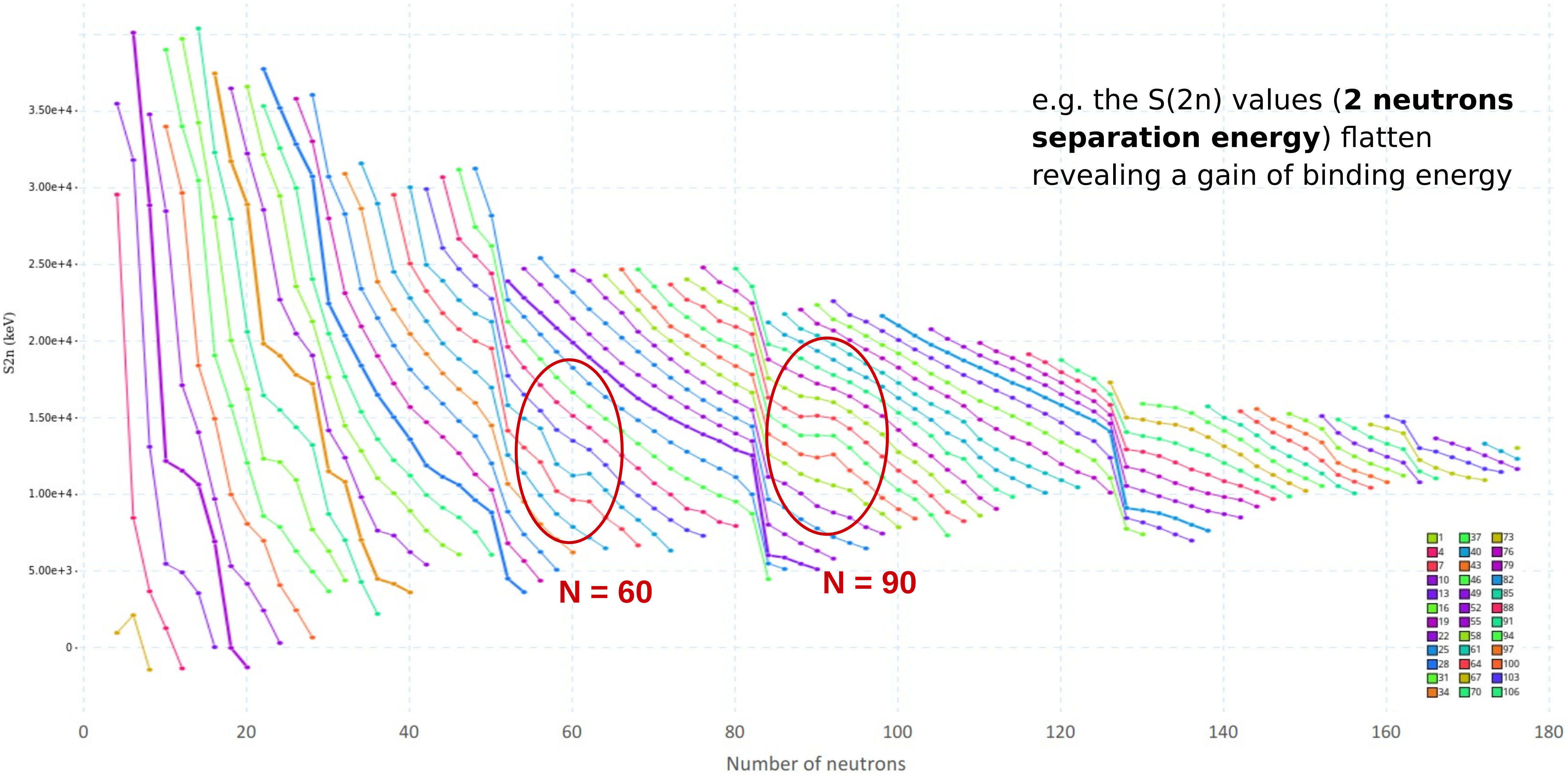

e.g. the S(2n) values (**2 neutrons separation energy**) flatten revealing a gain of binding energy

Shape evolution in neutron-rich nuclei around A=100

e.g. the **ratio R(4/2)** between the energies of the 4_1^+ and the 2_1^+ excited states suddenly increases

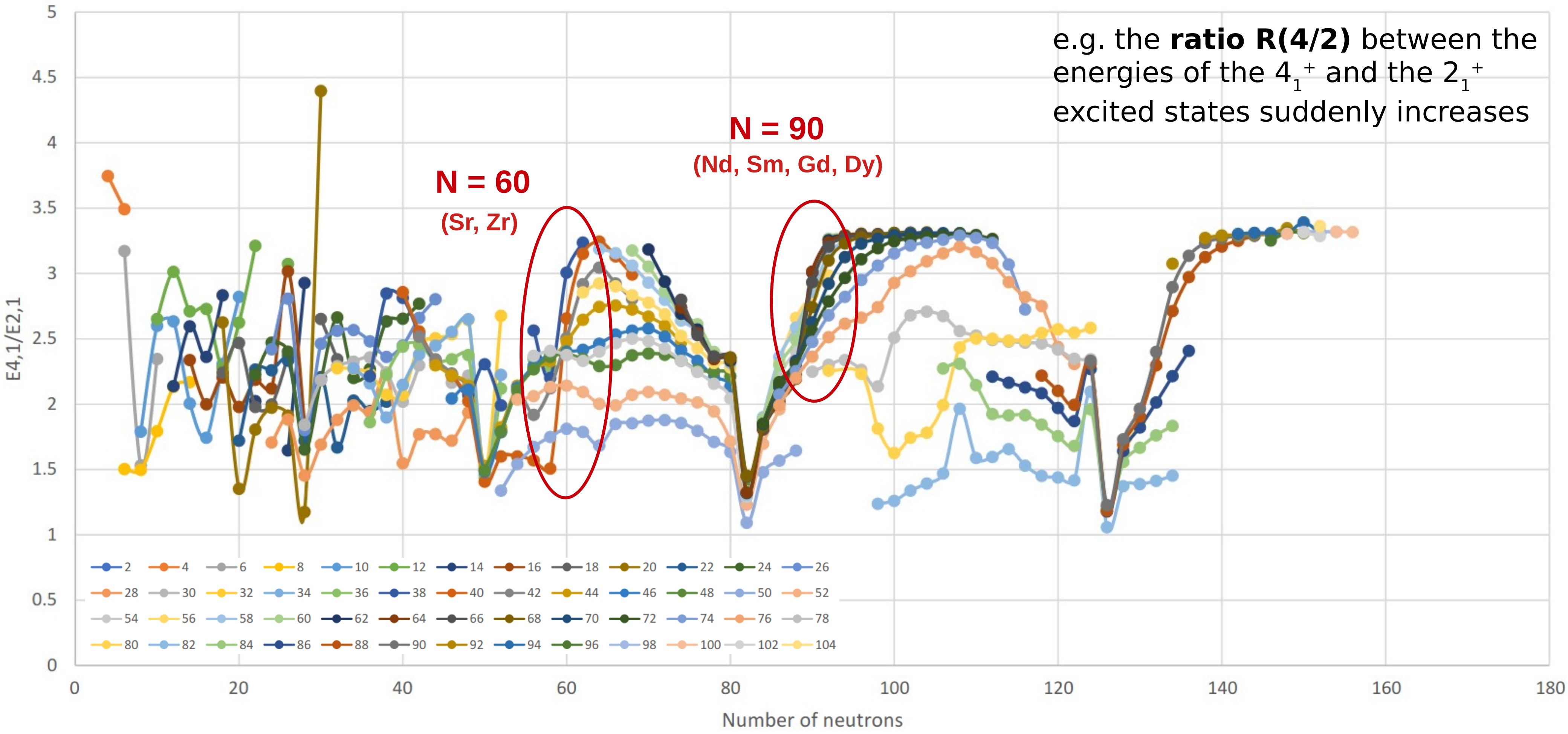

Shape evolution in neutron-rich nuclei around A=100

- **Drastic change** of 2^+ energies and B(E2) values as a function of N (and Z)

<u>Energy</u> of the first 2_1^+

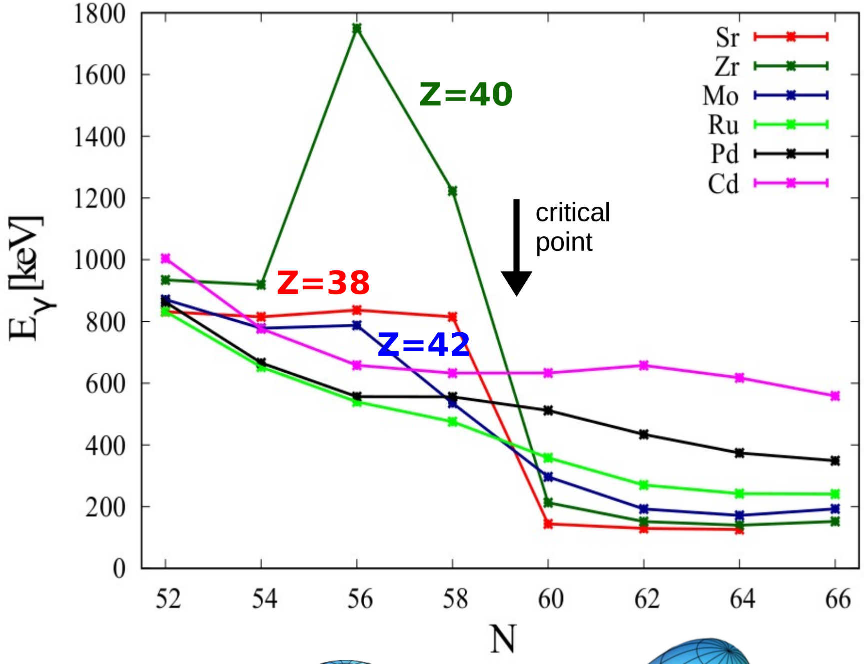

<u>Decay probability</u> B(E2; $2_1^+ \rightarrow 0_1^+$)

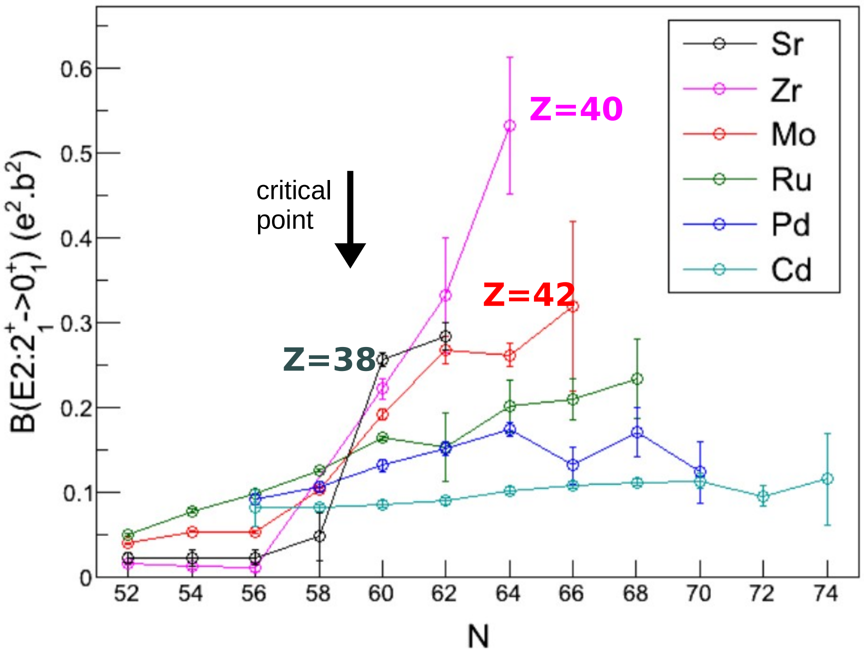

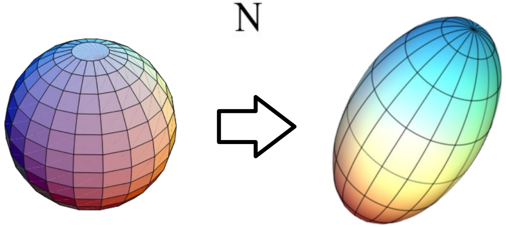

The strong dependence of nuclear properties on both N and Z makes the A~100 region an interesting test ground for various theoretical models.

Microscopic interpretation

- Federman, Pittel and co-workers pointed out for the first time a microscopic approach within the framework of the shell-model

P. Federman and S. Pittel, “Towards a unified microscopic description of nuclear deformation,” Phys. Lett. B 69, 385–388 (1977).

P. Federman, S. Pittel, and R. Campos, “Microscopic study of the shape transition in the zirconium isotopes,” Phys. Lett. B 82, 9–12 (1979).

P. Federman and S. Pittel, “Unified shell-model description of nuclear deformation,” Phys. Rev. C 20, 820–829 (1979).

P. Federman, S. Pittel, and A. Etchegoyen, “Quenching of the $2p_{1/2}2p_{3/2}$ proton spin-orbit splitting in the Sr Zr region,” Phys. Lett. B 140, 269–271 (1984).

K. Heyde, E. D. Kirchuk, and P. Federman, “Coexistence or strong-mixing of intruder 0+ states in even-even Zr nuclei,” Phys. Rev. C 38, 984–992 (1988).

A. Etchegoyen, P. Federman, and E. G. Vergini, “Importance of the neutron-proton interaction for Zr isotopes,” Phys. Rev. C 39, 1130–1133 (1989).

S. Pittel, P. Federman, G. E. Arenas Peris, R. F. Casten, and W.-T. Chou, “Semiempirical determination of effective p-n monopole matrix elements.” Phys. Rev. C 48, 1050 (1993).

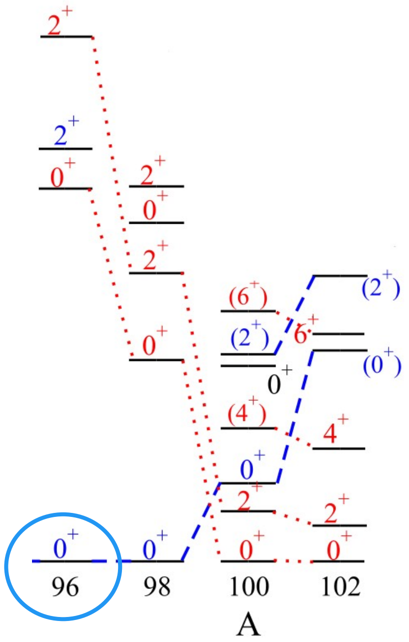

0_1^+ g.s. ^{96}Zr

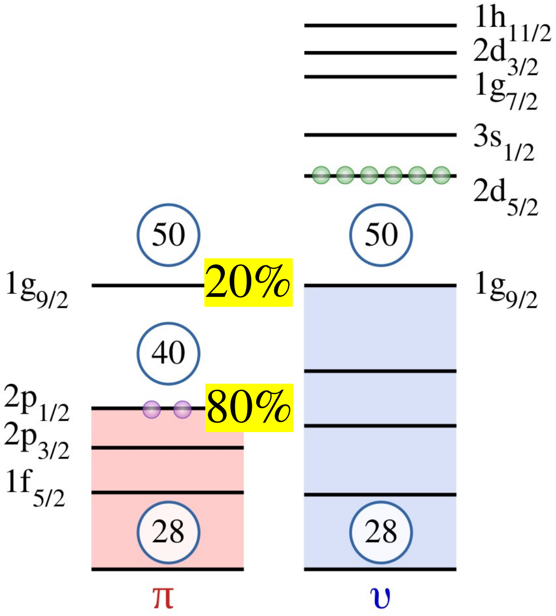

Microscopic interpretation

- Federman, Pittel and co-workers pointed out for the first time a microscopic approach within the framework of the shell-model

P. Federman and S. Pittel, “Towards a unified microscopic description of nuclear deformation,” Phys. Lett. B 69, 385–388 (1977).

P. Federman, S. Pittel, and R. Campos, “Microscopic study of the shape transition in the zirconium isotopes,” Phys. Lett. B 82, 9–12 (1979).

P. Federman and S. Pittel, “Unified shell-model description of nuclear deformation,” Phys. Rev. C 20, 820–829 (1979).

P. Federman, S. Pittel, and A. Etchegoyen, “Quenching of the $2p_{1/2}2p_{3/2}$ proton spin-orbit splitting in the Sr Zr region,” Phys. Lett. B 140, 269–271 (1984).

K. Heyde, E. D. Kirchuk, and P. Federman, “Coexistence or strong-mixing of intruder 0+ states in even-even Zr nuclei,” Phys. Rev. C 38, 984–992 (1988).

A. Etchegoyen, P. Federman, and E. G. Vergini, “Importance of the neutron-proton interaction for Zr isotopes,” Phys. Rev. C 39, 1130–1133 (1989).

S. Pittel, P. Federman, G. E. Arenas Peris, R. F. Casten, and W.-T. Chou, “Semiempirical determination of effective p-n monopole matrix elements.” Phys. Rev. C 48, 1050 (1993).

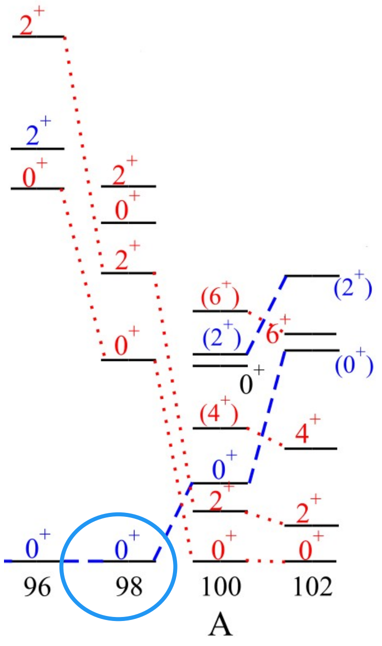

0_1^+ g.s. ^{98}Zr

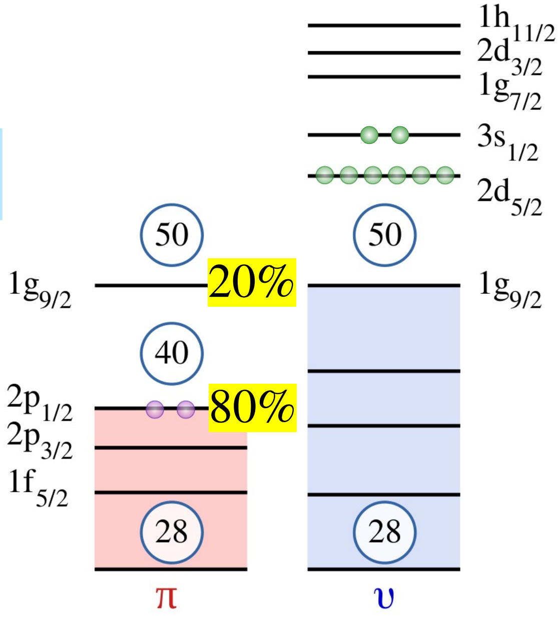

Microscopic interpretation

- Federman, Pittel and co-workers pointed out for the first time a microscopic approach within the framework of the shell-model

P. Federman and S. Pittel, “Towards a unified microscopic description of nuclear deformation,” Phys. Lett. B 69, 385–388 (1977).

P. Federman, S. Pittel, and R. Campos, “Microscopic study of the shape transition in the zirconium isotopes,” Phys. Lett. B 82, 9–12 (1979).

P. Federman and S. Pittel, “Unified shell-model description of nuclear deformation,” Phys. Rev. C 20, 820–829 (1979).

P. Federman, S. Pittel, and A. Etchegoyen, “Quenching of the $2p_{1/2}2p_{3/2}$ proton spin-orbit splitting in the Sr Zr region,” Phys. Lett. B 140, 269–271 (1984).

K. Heyde, E. D. Kirchuk, and P. Federman, “Coexistence or strong-mixing of intruder 0+ states in even-even Zr nuclei,” Phys. Rev. C 38, 984–992 (1988).

A. Etchegoyen, P. Federman, and E. G. Vergini, “Importance of the neutron-proton interaction for Zr isotopes,” Phys. Rev. C 39, 1130–1133 (1989).

S. Pittel, P. Federman, G. E. Arenas Peris, R. F. Casten, and W.-T. Chou, “Semiempirical determination of effective p-n monopole matrix elements.” Phys. Rev. C 48, 1050 (1993).

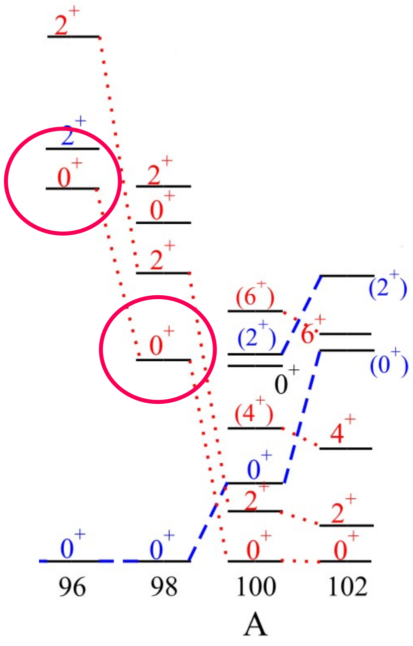

0_2^+ exc ^{98}Zr

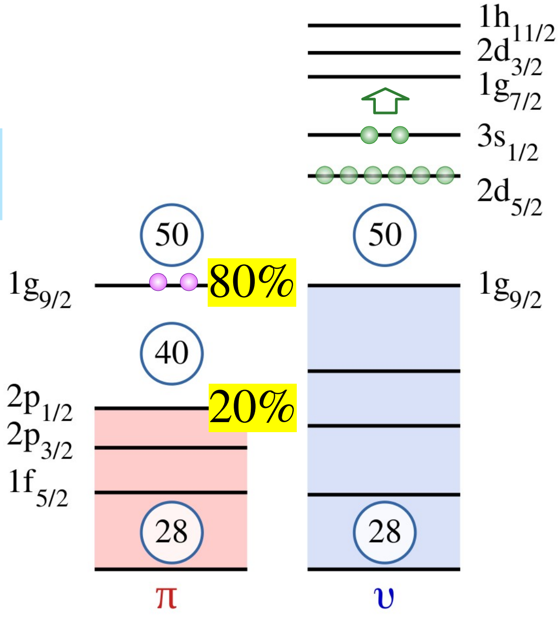

Microscopic interpretation

- Federman, Pittel and co-workers pointed out for the first time a microscopic approach within the framework of the shell-model

P. Federman and S. Pittel, "Towards a unified microscopic description of nuclear deformation," Phys. Lett. B 69, 385–388 (1977).

P. Federman, S. Pittel, and R. Campos, "Microscopic study of the shape transition in the zirconium isotopes," Phys. Lett. B 82, 9–12 (1979).

P. Federman and S. Pittel, "Unified shell-model description of nuclear deformation," Phys. Rev. C 20, 820–829 (1979).

P. Federman, S. Pittel, and A. Etchegoyen, "Quenching of the $2p_{1/2}2p_{3/2}$ proton spin-orbit splitting in the Sr Zr region," Phys. Lett. B 140, 269–271 (1984).

K. Heyde, E. D. Kirchuk, and P. Federman, "Coexistence or strong-mixing of intruder 0+ states in even-even Zr nuclei," Phys. Rev. C 38, 984–992 (1988).

A. Etchegoyen, P. Federman, and E. G. Vergini, "Importance of the neutron-proton interaction for Zr isotopes," Phys. Rev. C 39, 1130–1133 (1989).

S. Pittel, P. Federman, G. E. Arenas Peris, R. F. Casten, and W.-T. Chou, "Semiempirical determination of effective p-n monopole matrix elements." Phys. Rev. C 48, 1050 (1993).

The possibility that the lowering of the first excited 0^+ level might be closely related to the observed shape transition has motivated several efforst to understand its origin [5,6]. A coexistence of deformed and spherical shapes has been suggested for ^{98}Zr,

- Lowering of excited 0+ states: shape transition and shape coexistence

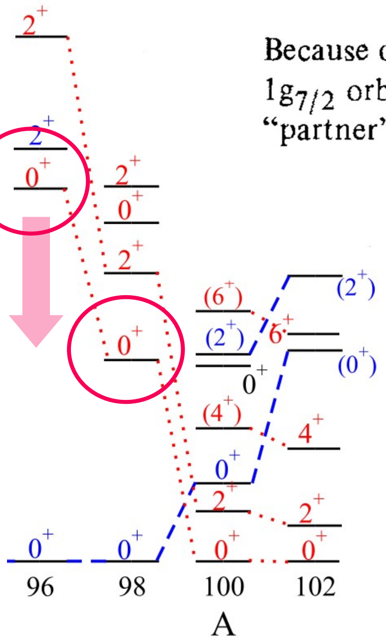

0_2^+ exc ^{98}Zr

Because of the possibility of neutrons filling the $1g_{7/2}$ orbit, the neutron–proton interaction between "partner" orbits becomes very strong

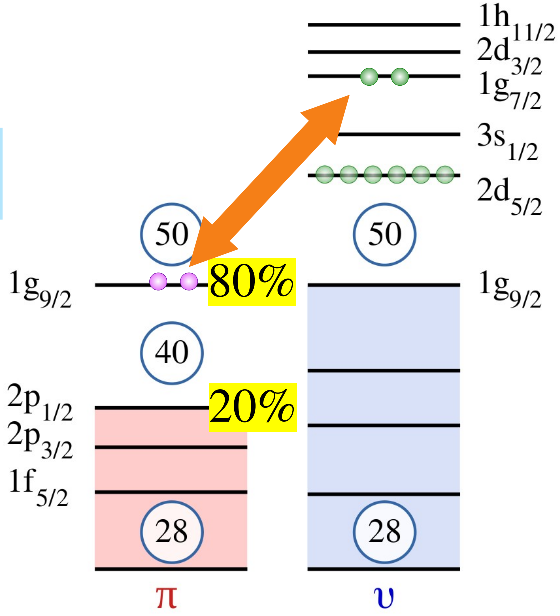

Configuration A

Configuration B

- The drastic shape transition originates from the crossing of the normal configuration with an intruder configuration having a very different degree of deformation.
- Shape coexistence is predicted and observed in the transitional region, for ^{96}Zr, ^{98}Zr, ^{100}Zr.

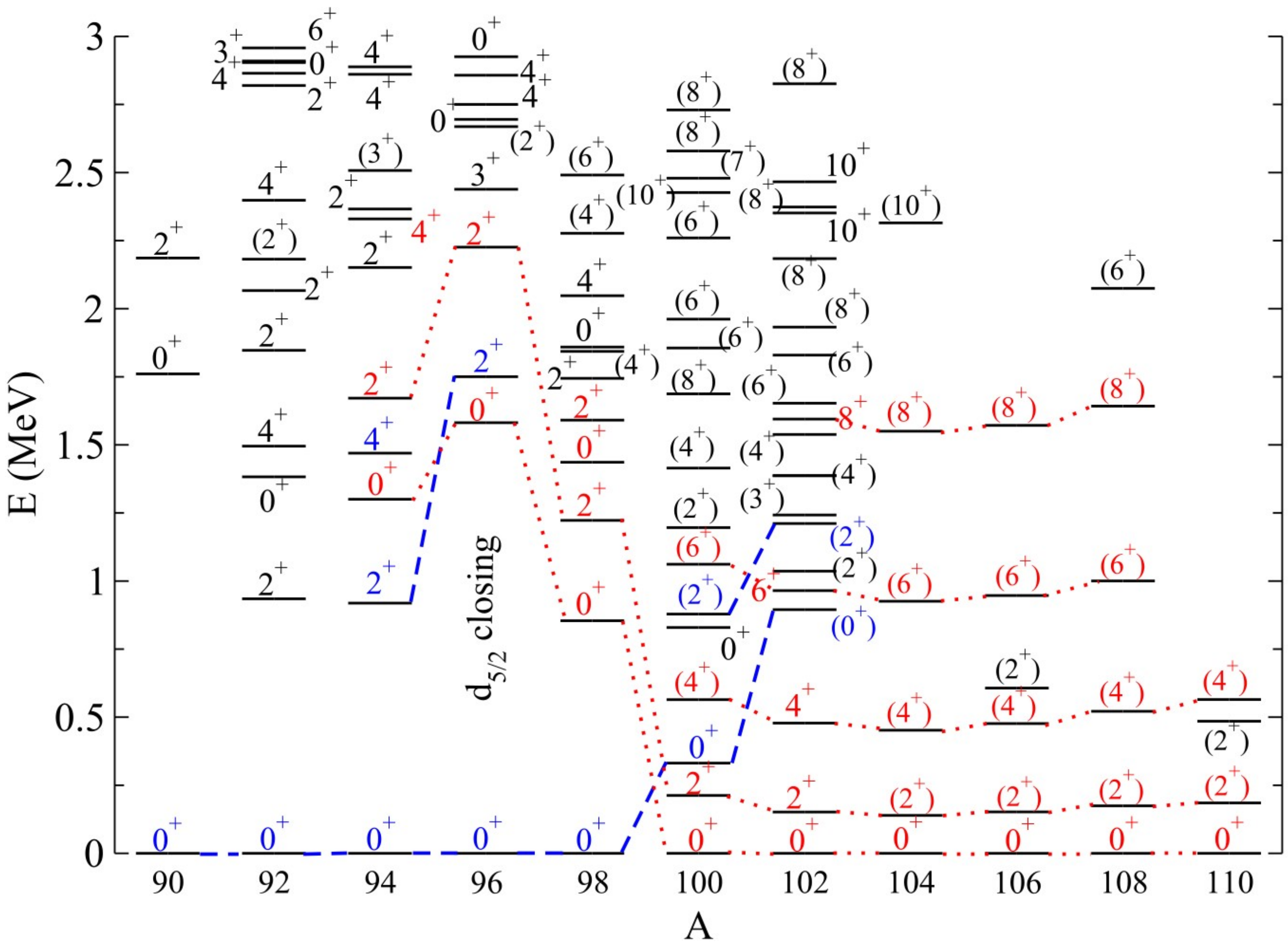

J. E. García-Ramos and K. Heyde, Phys. Rev. C 102, 054333 (2020).

- Large theoretical effort have been invested to study this phenomenon

generator coordinate method (GCM):
J. Skalski, P.-H. Heenen, and P. Bonche, Nucl. Phys. A 559, 221 (1993).
J.-P. Delaroche et al., PRC 81, 014303 (2010).

macroscopic-microscopic method:
J. Skalski, S. Mizutory, and W. Nazarewicz, Nucl. Phys. A 617, 282 (1997).

Shell Model:
P. G. Reinhard, et al., PRC 60, 014316 (1999).
A. Holt, T. Engeland, M. Hjorth-Jensen, and E. Osnes, PRC 61, 064318 (2000).
K. Sieja, F. Nowacki, K. Langanke, and G. Martínez-Pinedo, PRC 79, 064310 (2009).
Y.-X. Liu et al., Nucl. Phys. A 858, 11 (2011).

Shell Model Monte Carlo
C. Özen and D. J. Dean, PRC 73, 014302 (2006).

Monte Carlo Shell Model:
T. Togashi, Y. Tsunoda, T. Otsuka and N. Shimizu, PRL 117, 172502 (2016).

interacting boson model (IBM & IBM-CM):
J. E. García-Ramos, et al., Eur. Phys. J. A 26, 221 (2005).
M. Böyükata, P. Van Isacker and İ. Uluer, J. Phys. G: Nucl. Part. Phys. 37, 105102 (2010).
K. Nomura, R. Rodríguez-Guzmán, and L. M. Robledo, PRC 94, 044314 (2016).
A. Vitturi, L. Fortunato, I. Inci, and J.A. Lay, JPS Conf. Proc. 23, 012013 (2018).
J. E. García-Ramos and K. Heyde, PRC 102, 054333 (2020).
N. Gavrielov, A. Leviatan, and F. Iachello, PRC 105, 014305 (2022).

Hartree-Fock (HF) and Hartree-Fock-Bogoliubov (HFB) models:
R. Rodríguez-Guzmán et al., PLB 691, 202 (2010).
S. Miyahara and H. Nakada, PRC 98, 064318 (2018).

Excited Vampir model:
A. Petrovici, K.W. Schmid and A. Faessler, J. Phys.: 312, 092051 (2011).

covariant density functional (DF) theory:
J. Xiang et al., Nucl. Phys. A 873, 1 (2012).

......

P. Singh et al., Phys. Rev. Lett. 121 (19), 192501 (2018).

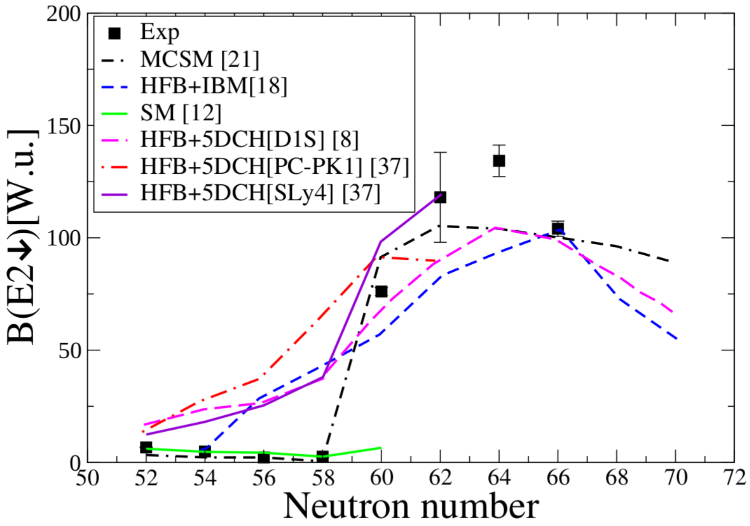

- Large theoretical effort have been invested to study this phenomenon

generator coordinate method (GCM):
J. Skalski, P.-H. Heenen, and P. Bonche, Nucl. Phys. A 559, 221 (1993).
J.-P. Delaroche et al., PRC 81, 014303 (2010).

macroscopic-microscopic method:
J. Skalski, S. Mizutory, and W. Nazarewicz, Nucl. Phys. A 617, 282 (1997).

Shell Model:
P. G. Reinhard, et al., PRC 60, 014316 (1999).
A. Holt, T. Engeland, M. Hjorth-Jensen, and E. Osnes, PRC 61, 064318 (2000).
K. Sieja, F. Nowacki, K. Langanke, and G. Martínez-Pinedo, PRC 79, 064310 (2009).
Y.-X. Liu et al., Nucl. Phys. A 858, 11 (2011).

Shell Model Monte Carlo
C. Özen and D. J. Dean, PRC 73, 014302 (2006).

Monte Carlo Shell Model:
T. Togashi, Y. Tsunoda, T. Otsuka and N. Shimizu, PRL 117, 172502 (2016).

interacting boson model (IBM & IBM-CM):
J. E. García-Ramos, et al., Eur. Phys. J. A 26, 221 (2005).
M. Böyükata, P. Van Isacker and İ. Uluer, J. Phys. G: Nucl. Part. Phys. 37, 105102 (2010).
K. Nomura, R. Rodríguez-Guzmán, and L. M. Robledo, PRC 94, 044314 (2016).
A. Vitturi, L. Fortunato, I. Inci, and J.A. Lay, JPS Conf. Proc. 23, 012013 (2018).
J. E. García-Ramos and K. Heyde, PRC 102, 054333 (2020).
N. Gavrielov, A. Leviatan, and F. Iachello, PRC 105, 014305 (2022).

Hartree-Fock (HF) and Hartree-Fock-Bogoliubov (HFB) models:
R. Rodríguez-Guzmán et al., PLB 691, 202 (2010).
S. Miyahara and H. Nakada, PRC 98, 064318 (2018).

Excited Vampir model:
A. Petrovici, K.W. Schmid and A. Faessler, J. Phys.: 312, 092051 (2011).

covariant density functional (DF) theory:
J. Xiang et al., Nucl. Phys. A 873, 1 (2012).

......

- Monte Carlo Shell Model (2016)

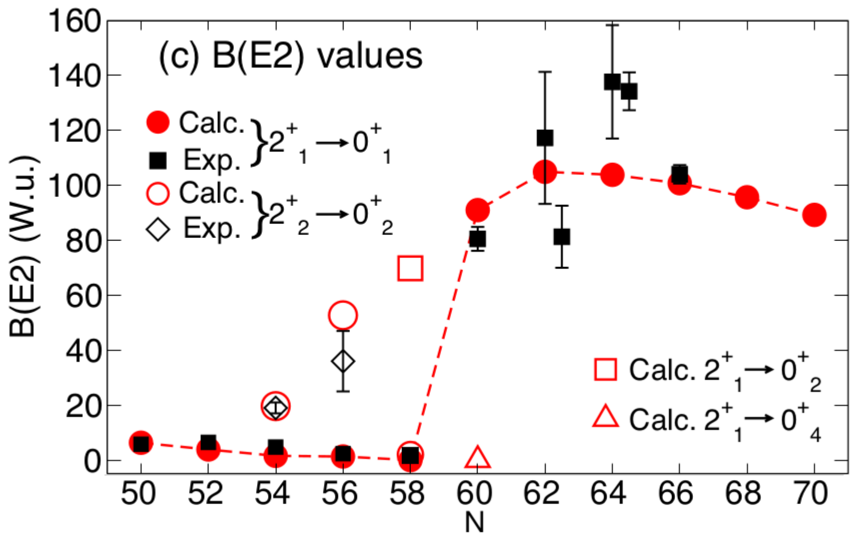

- Large theoretical effort have been invested to study this phenomenon

generator coordinate method (GCM):
J. Skalski, P.-H. Heenen, and P. Bonche, Nucl. Phys. A 559, 221 (1993).
J.-P. Delaroche et al., PRC 81, 014303 (2010).

macroscopic-microscopic method:
J. Skalski, S. Mizutory, and W. Nazarewicz, Nucl. Phys. A 617, 282 (1997).

Shell Model:
P. G. Reinhard, et al., PRC 60, 014316 (1999).
A. Holt, T. Engeland, M. Hjorth-Jensen, and E. Osnes, PRC 61, 064318 (2000).
K. Sieja, F. Nowacki, K. Langanke, and G. Martínez-Pinedo, PRC 79, 064310 (2009).
Y.-X. Liu et al., Nucl. Phys. A 858, 11 (2011).

Shell Model Monte Carlo
C. Özen and D. J. Dean, PRC 73, 014302 (2006).

Monte Carlo Shell Model:
T. Togashi, Y. Tsunoda, T. Otsuka and N. Shimizu, PRL 117, 172502 (2016).

interacting boson model (IBM & IBM-CM):
J. E. García-Ramos, et al., Eur. Phys. J. A 26, 221 (2005).
M. Böyükata, P. Van Isacker and İ. Uluer, J. Phys. G: Nucl. Part. Phys. 37, 105102 (2010).
K. Nomura, R. Rodríguez-Guzmán, and L. M. Robledo, PRC 94, 044314 (2016).
A. Vitturi, L. Fortunato, I. Inci, and J.A. Lay, JPS Conf. Proc. 23, 012013 (2018).
J. E. García-Ramos and K. Heyde, PRC 102, 054333 (2020).
N. Gavrielov, A. Leviatan, and F. Iachello, PRC 105, 014305 (2022).

Hartree-Fock (HF) and Hartree-Fock-Bogoliubov (HFB) models:
R. Rodríguez-Guzmán et al., PLB 691, 202 (2010).
S. Miyahara and H. Nakada, PRC 98, 064318 (2018).

Excited Vampir model:
A. Petrovici, K.W. Schmid and A. Faessler, J. Phys.: 312, 092051 (2011).

covariant density functional (DF) theory:
J. Xiang et al., Nucl. Phys. A 873, 1 (2012).

......

- Interacting Boson Model with Configuration Mixing (2022)

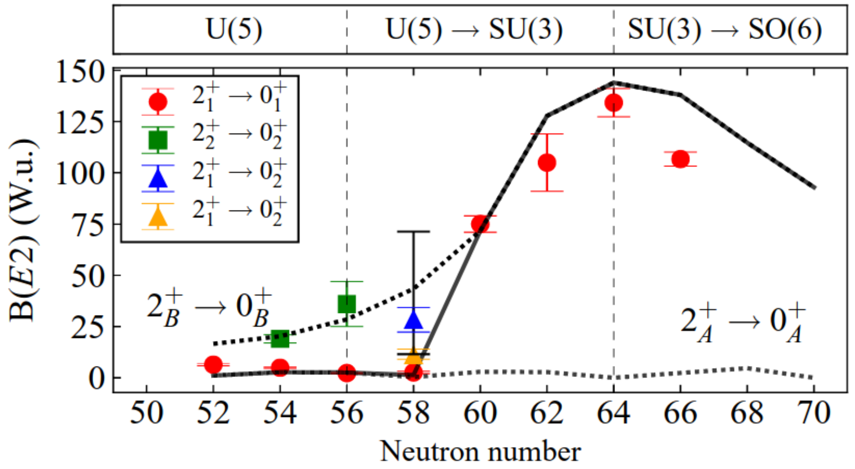

- INTRODUCTION :
  - Deformation and shapes in nuclei.
  - How can we study them from experiments?
  - Quantum phase transition in Zr isotopes.
- EXPERIMENT :
  - The experimental setup AGATA+VAMOS+plunger.
  - Lifetime measurements with the RDDS technique.
- ANALYSIS :
  - Lifetime results for 98-104Zr.
  - Comparison with theoretical predictions: MCSM, IBM-CM and SCCM-HFB.

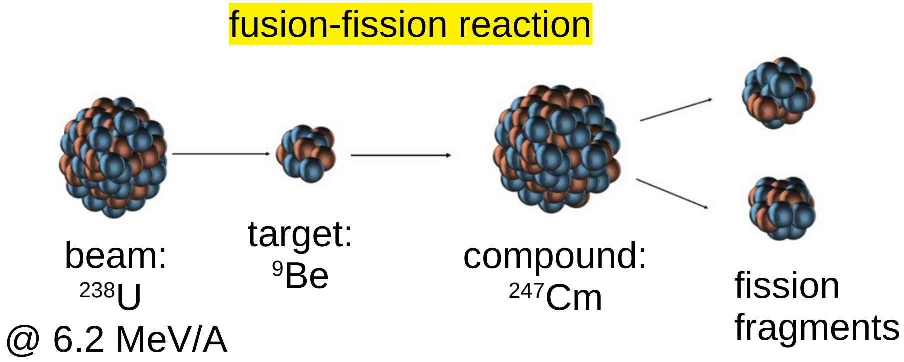
fusion-fission reaction
beam:
238U
@ 6.2 MeV/A
target:
9Be
compound:
247Cm
fission
fragments

fusion-fission reaction

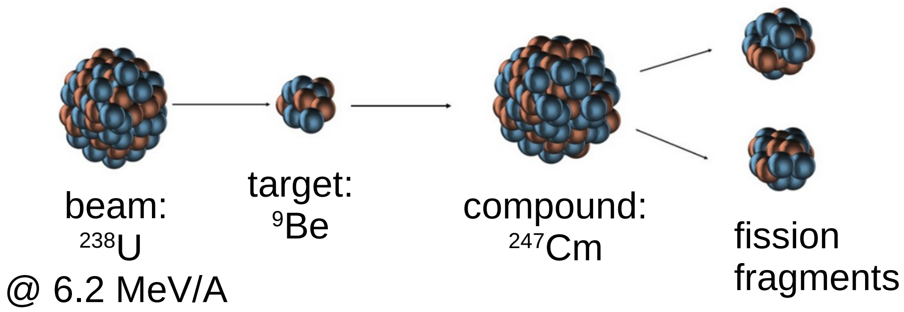

VAMOS large acceptance magnetic spectrometer

fragment identification based on atomic number Z, mass M and charge Q

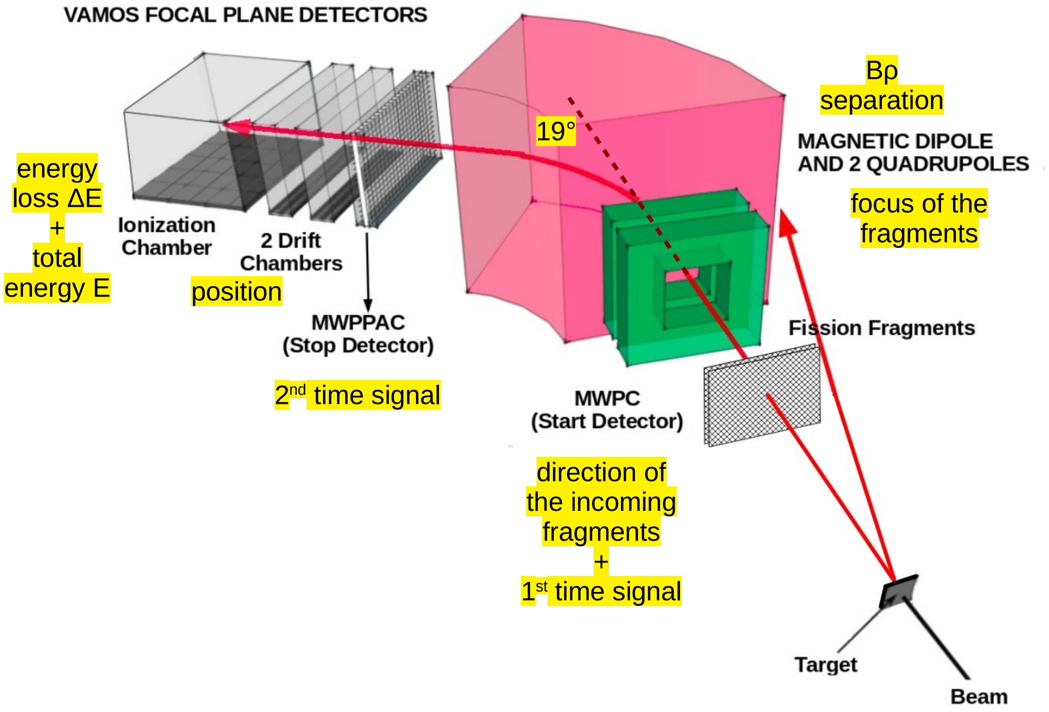

VAMOS large acceptance magnetic spectrometer

fragment identification based on atomic number Z, mass M and charge Q

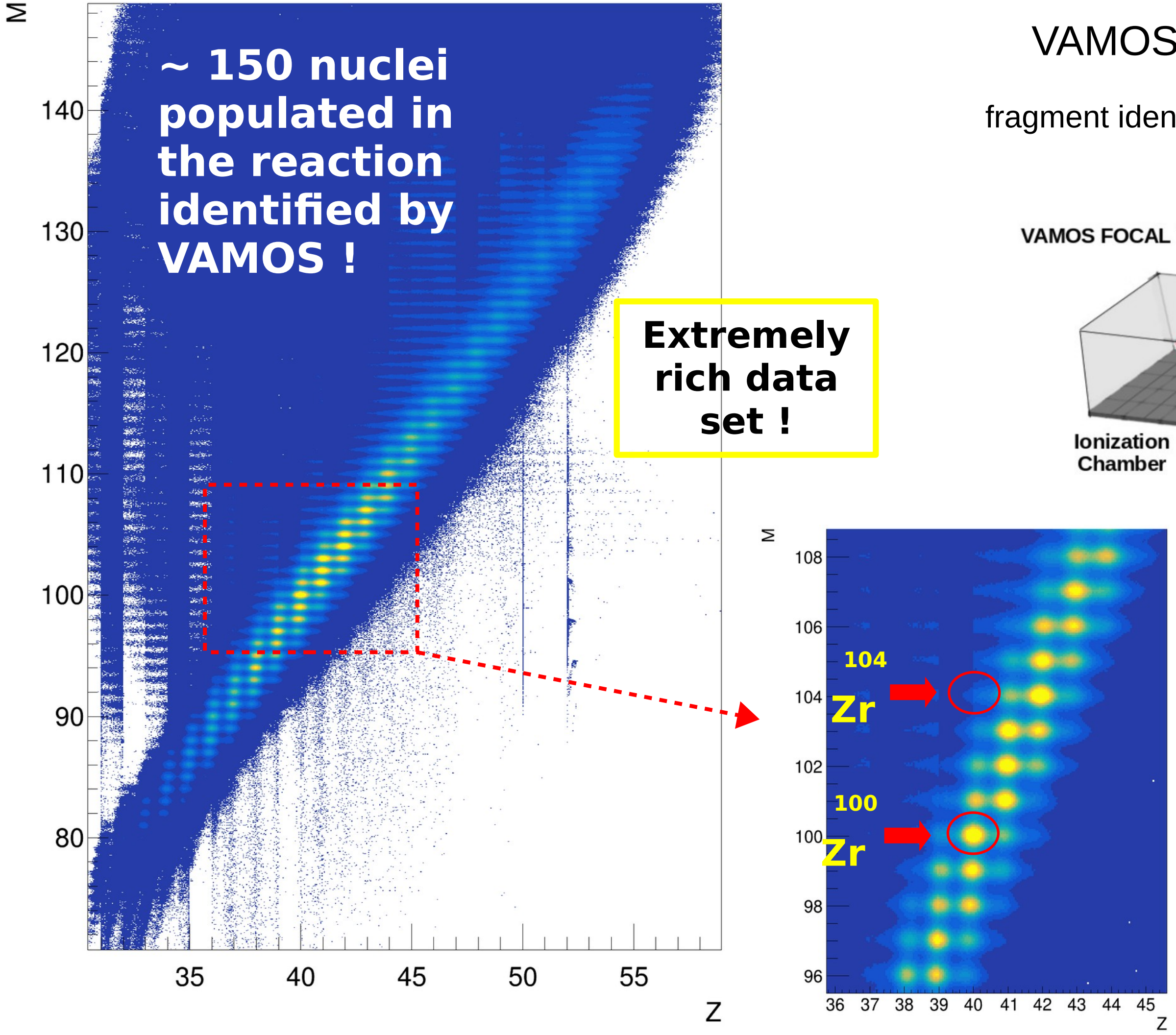

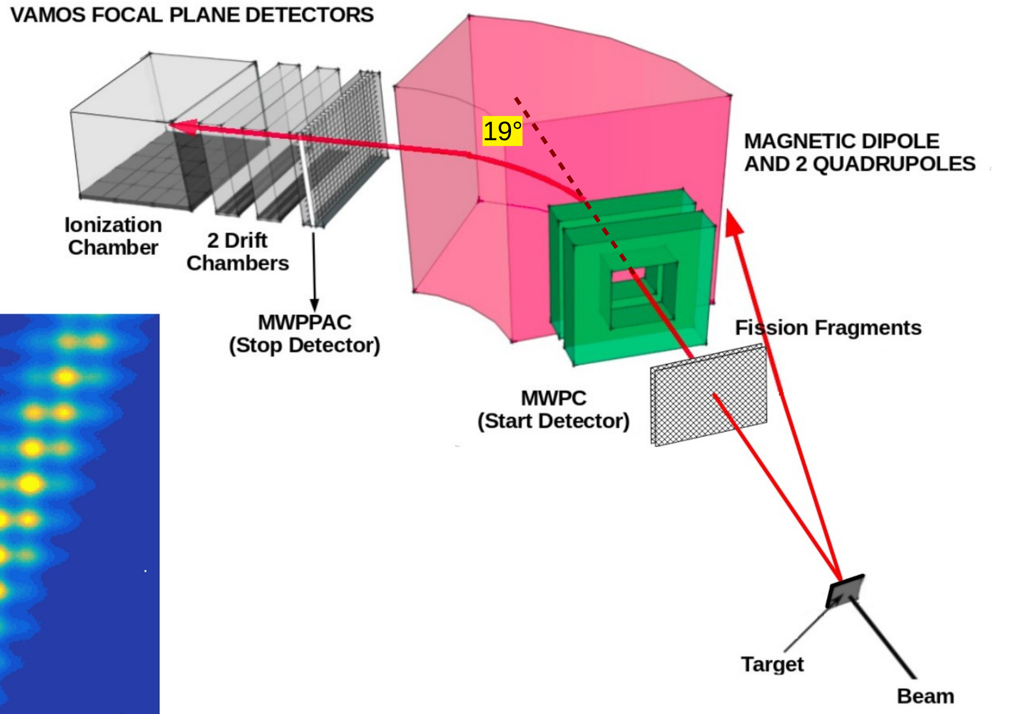

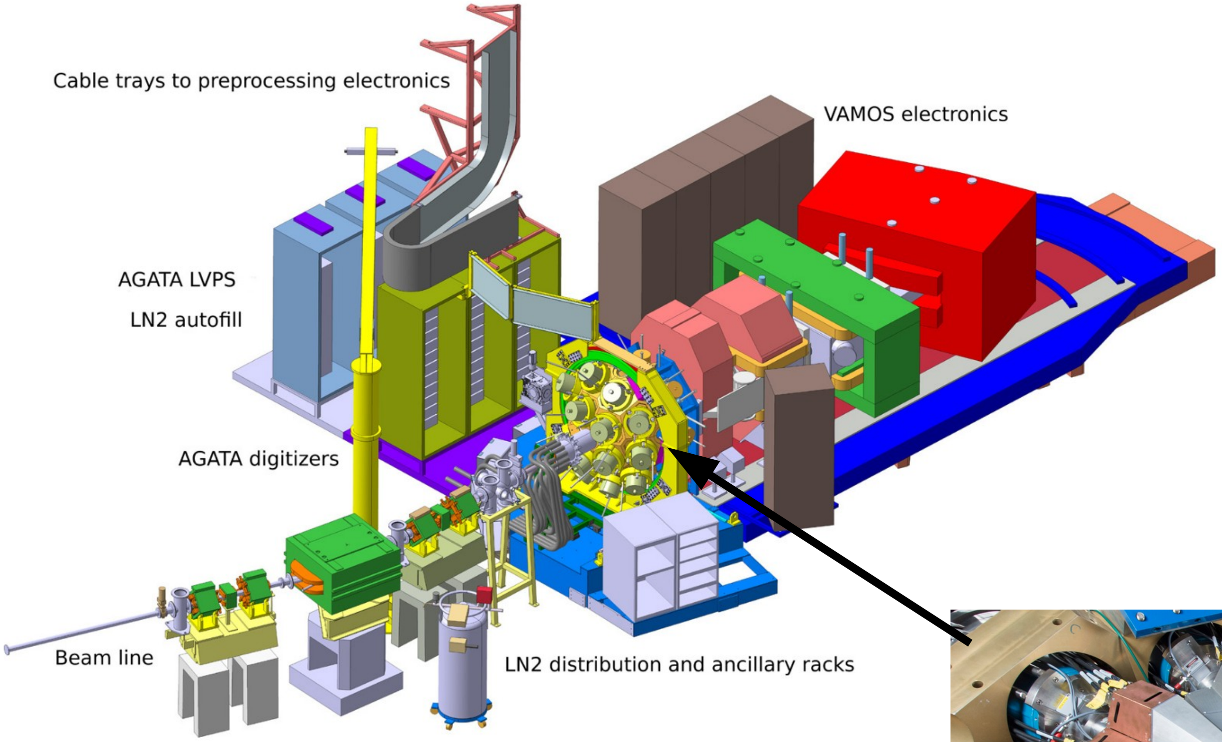

Advanced Gamma Tracking Array

Excellent energy resolution of HPGe detectors
+
unprecedented photo-peak efficiency
+
Pulse Shape Analysis (PSA) and γ-ray tracking

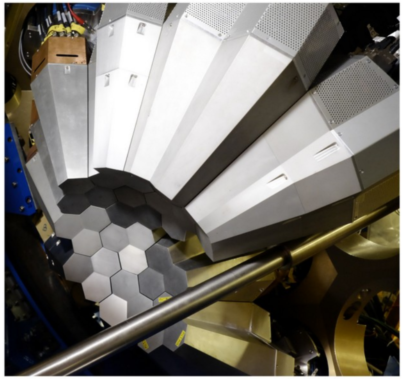

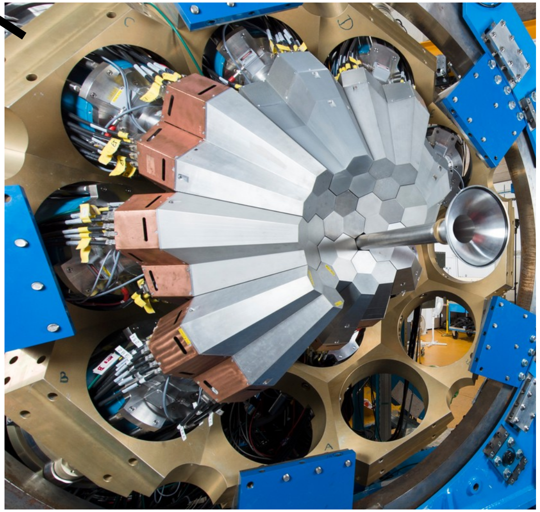

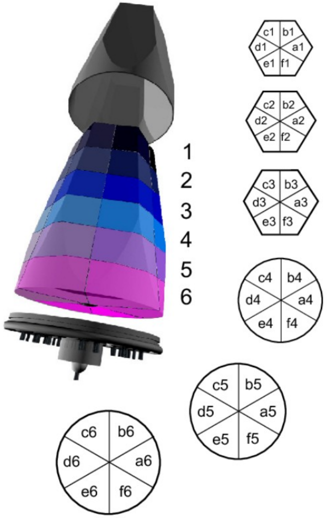

Recoil Distance Doppler Shift technique

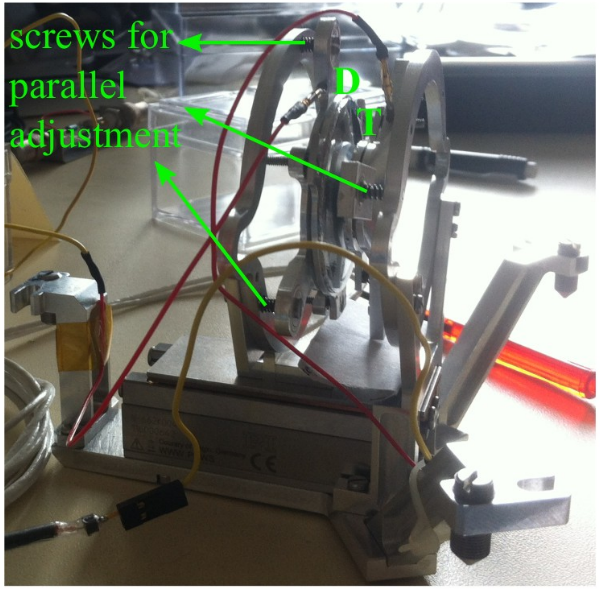

OUPS
Orsay Universal Plunger System

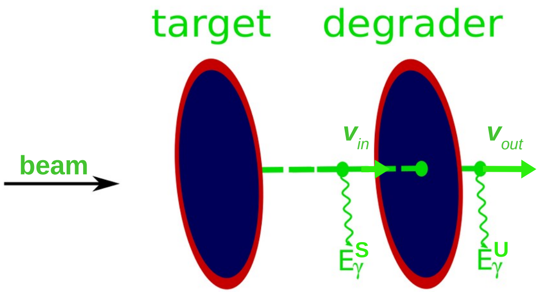

E_γ^S : shifted energy
E_γ^U : un-shifted energy

Recoil Distance Doppler Shift technique

- the energy of the γ ray emitted in-flight is Doppler shifted:

$$E = E_0 \frac{\sqrt{1-\beta^2}}{1-\beta\cos\Theta}$$

recoil velocity

angle of emission

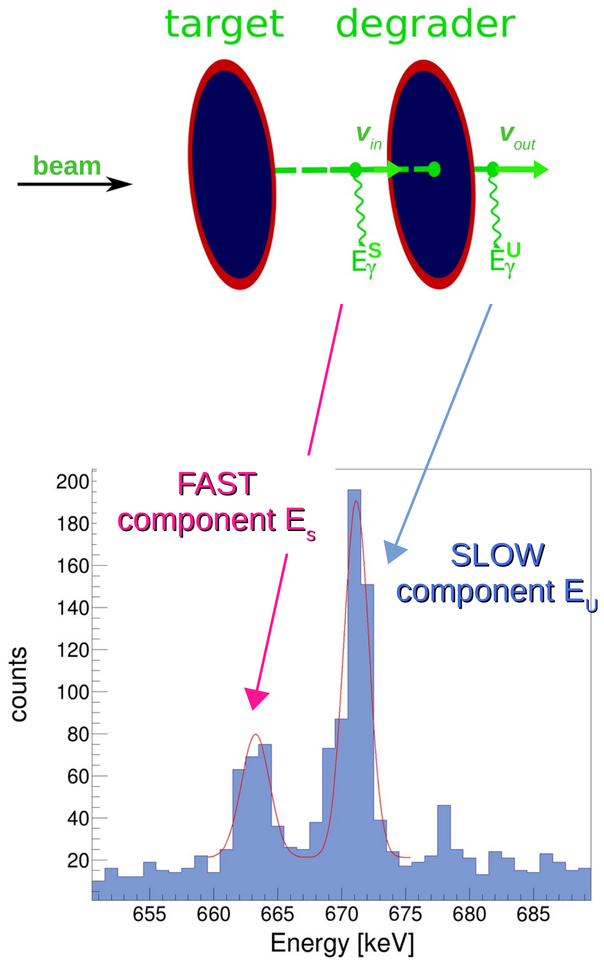

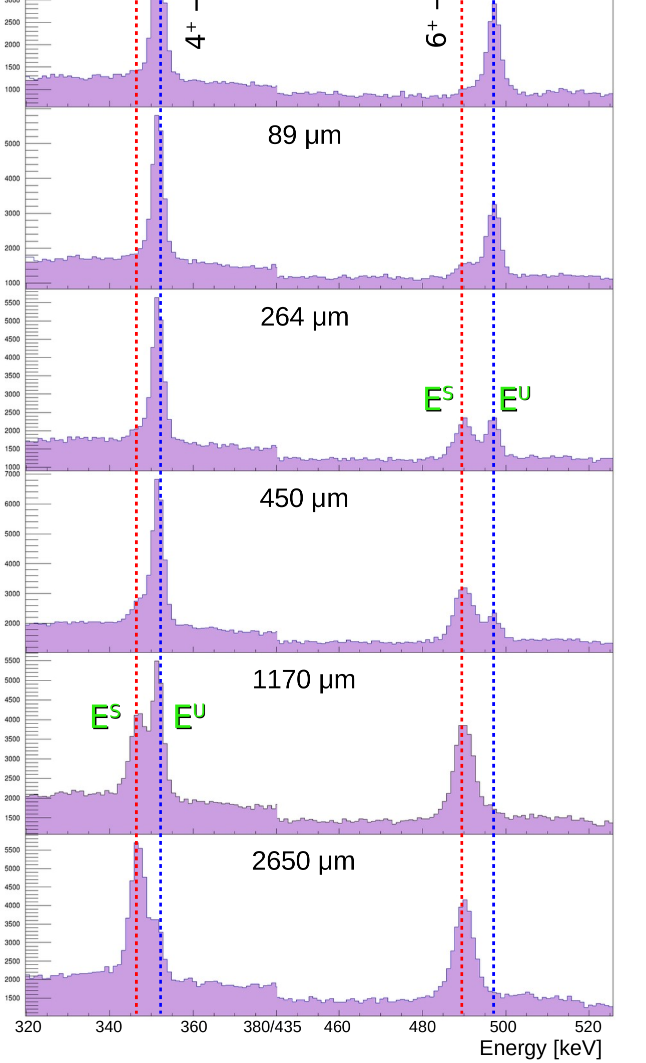

Decay Curve Method DCM

- the evolution of fast and slow components as a function of the distance provides the lifetime of the state

- simple two-level case:

$$n(t) = N_0 e^{-\frac{t}{\tau}}$$

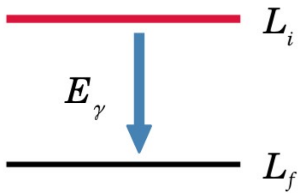

ratio R for the $4^+ \rightarrow 2^+$ transition in ^{100}Zr

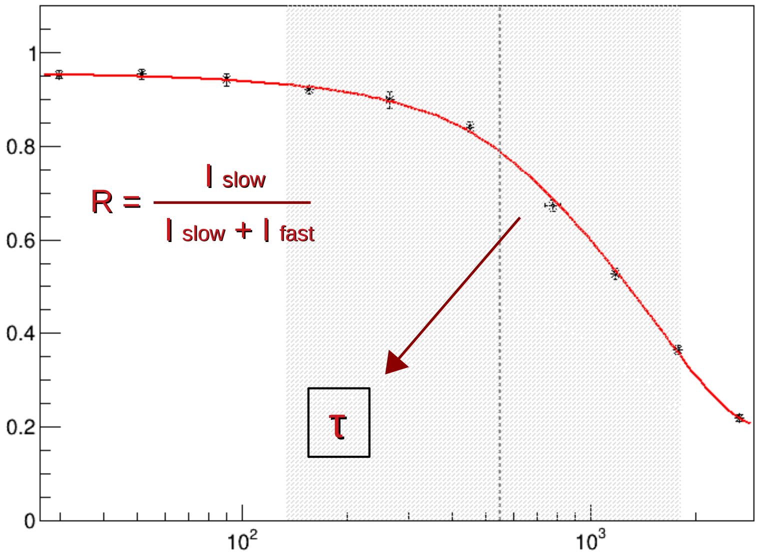

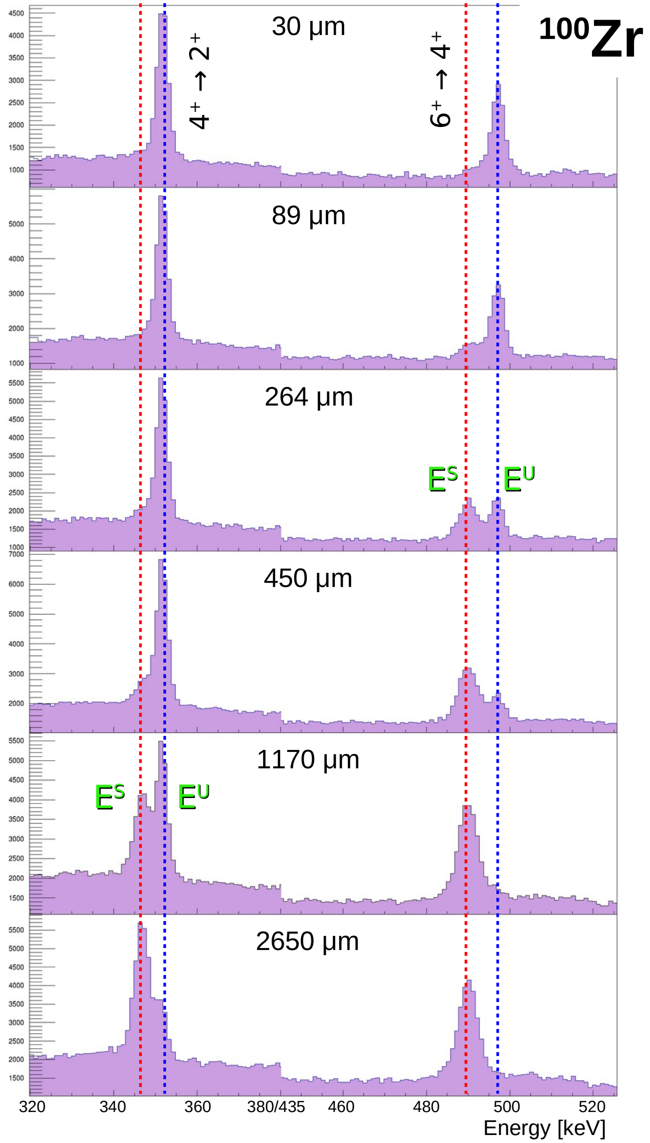

Decay Curve Method DCM

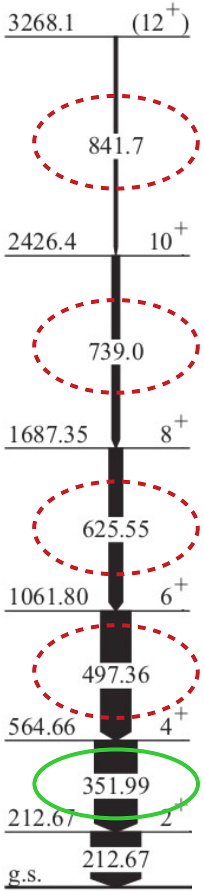

ratio R for the $4^+ \rightarrow 2^+$ transition in ^{100}Zr

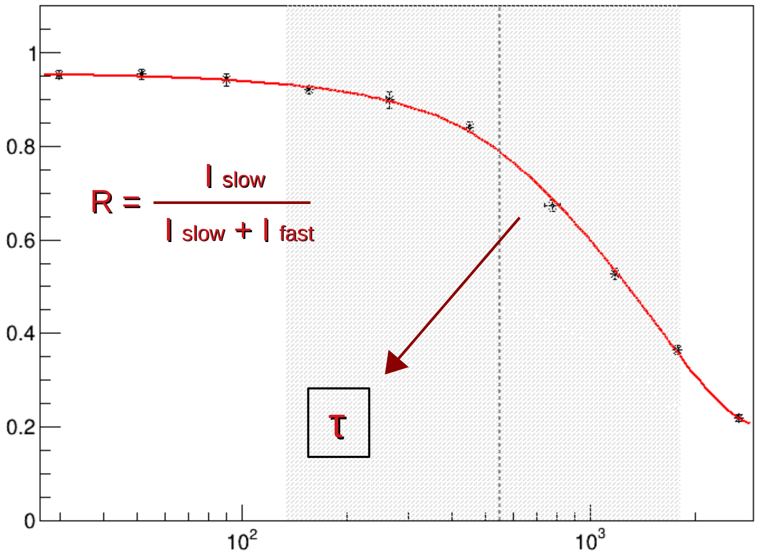

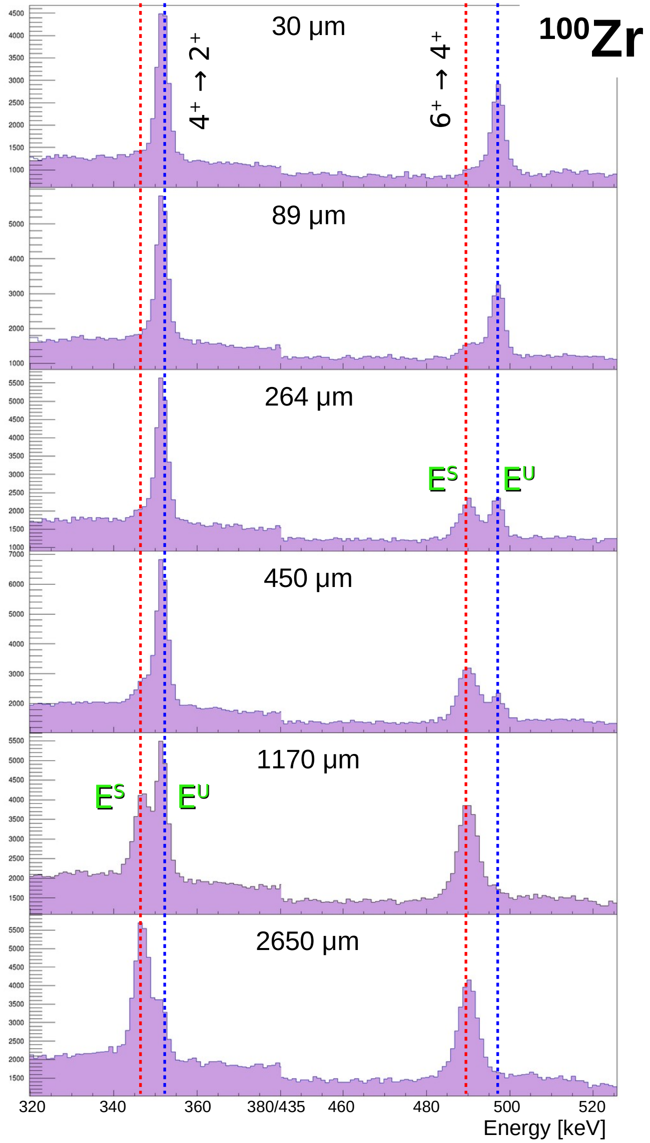

- using the Bateman equation as solution :

$$n_i(t) = \sum_{k=1}^{i} \left[n_k(0) \times \left(\prod_{j=k}^{i-1} \lambda_j \right) \times \left(\sum_{j=k}^{i} \frac{e^{-\lambda_j t}}{\prod_{p=k, p\neq j}^{i} (\lambda_p - \lambda_j)} \right) \right]$$

Differential Decay Curve Method DDCM

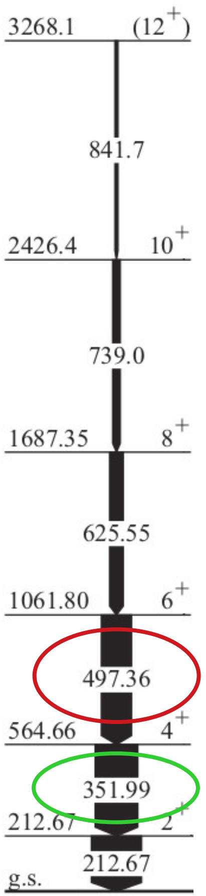

- Lifetime are analyzed with the **Differential Decay Curve Method** (DDCM) :
  - it deal with feeding problems
  - existence of a sensitive region
  - no assumption on the fitting curve shape
  - absolute distances are not needed

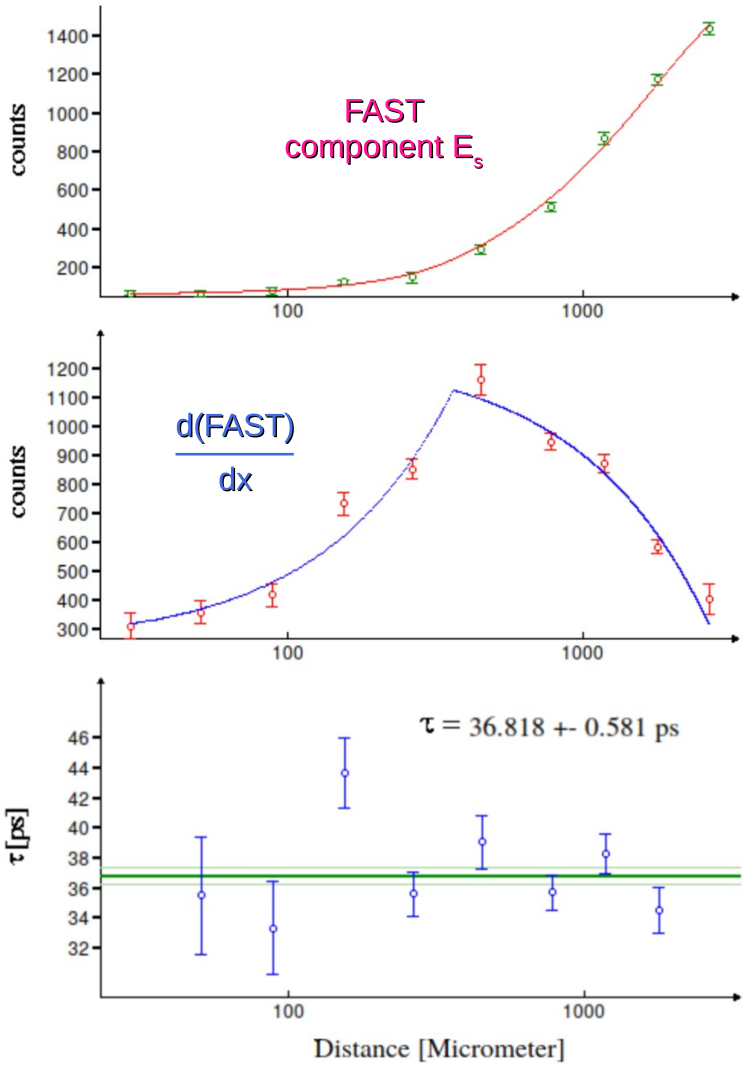

A. Dewald et al., Prog. Part. Nucl. Phys. 679, 786 (2012).
A. Dewald, S. Harissopulos, P. von Brentano, Z. Phys. A 334 (1989) 163.

Differential Decay Curve Method DDCM

- Lifetime in single γ measurements are analyzed with the DDCM by using the following experimental information:
  - the fast (S) and the slow (U) components of the transition A depopulating the state of interest L_i
  - the fast and the slow components of all observed feeding transitions B_j in the γ-rays spectrum (the α coefficient take into account the feeding contribution form all B_j in the lifetime calculation).
  - the velocity of the recoiling fragment before the target v_{in}.

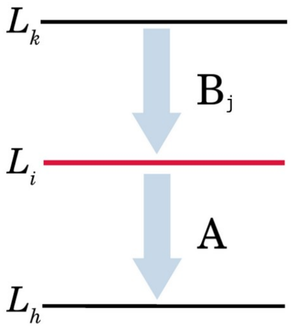

$$\tau(x_p) = \frac{-A^U(x_p) + \sum_j b_j \alpha_j B_j^U(x_p)}{v_{in} \frac{dA^U(x_p)}{dx}} \qquad \alpha_j(x_p) = \frac{B_j^U(x_p) + B_j^S(x_p)}{A^U(x_p) + A^S(x_p)} \cdot \frac{\epsilon_A}{\epsilon_B}$$

- Lifetime in coincidence γγ are analyzed with the DDCM by gating in the shifted component of a direct feeding transition B of the state of interest. No other information about the feeding are needed

$$\tau(x_p) = \frac{\{A_S, B_U\}(x_p)}{\frac{d}{dx}\{A_S, B_S\}(x_p)} \cdot \frac{1}{\beta c}$$

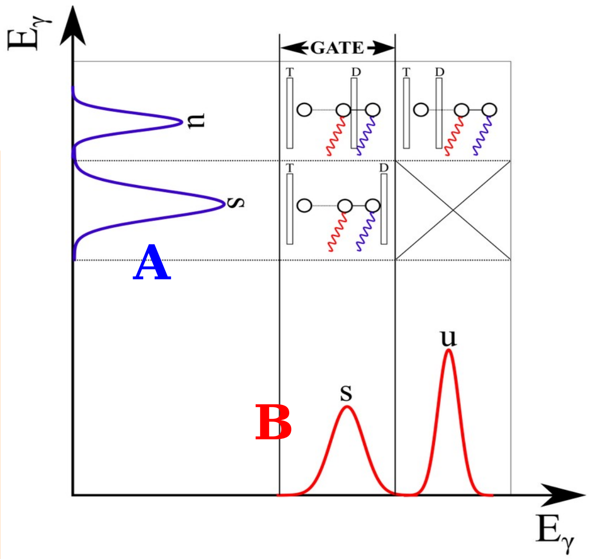

- INTRODUCTION :
    - Deformation and shapes in nuclei.
    - How can we study them from experiments?
    - Quantum phase transition in Zr isotopes.
- EXPERIMENT :
    - The experimental setup AGATA+VAMOS+plunger.
    - Lifetime measurements with the RDDS technique.
- ANALYSIS :
    - Lifetime results for 98-104Zr.
    - Comparison with theoretical predictions: MCSM, IBM-CM and SCCM-HFB.

Lifetime measurements in 100Zr

- Preliminary results: lifetime in gamma single and gamma-gamma coincidence.
- Comparison with previous results for the levels 4^+, 6^+, 8^+, 10^+ of the yrast band :

→ The adopted value for the 4^+ may be overestimated.
→ The 6^+ and 8^+ adopted lifetimes also result larger.
} unseen feeding ?

→ Measurements in γγ gives shorter lifetime for the 4^+, as expected.

→ The lifetime of the 8^+ is accurate in single γ due to the short-living feeding.

PRELIMINARY

Jπ	Energy [keV]	τ [ps] adopted*	τ [ps] single γ	τ [ps] coincid γγ
2+	*212.7*	574 (15)	/	/
4+	*352.0*	53.4 (6)	36.9 (6) **	**34 (3)**
6+	*497.4*	7.5 (1.6)	6.1 (3)	**6.4 (8)**
8+	*625.6*	2.5 (2)	1.3 (2)	**1.7 (4)**
10+	*739.0*	0.53 (6)	**0.7 (2)**	/

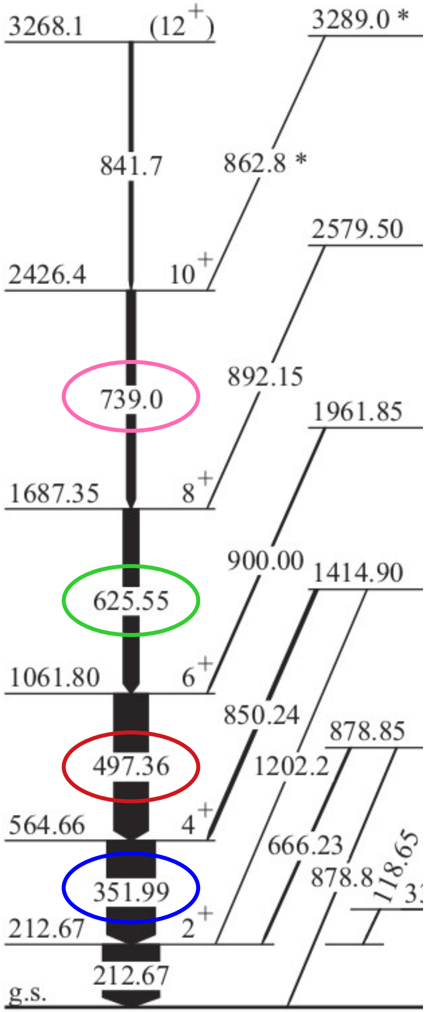

* EVALUATED NNDC, https://www.nndc.bnl.gov/nudat3/

** The feeding transition at 850.2 keV is not considered : difficult to resolve its shifted component from the 841.7 keV 12+ → 10+.

Lifetime measurements in 102Zr

- Preliminary results: lifetime in gamma single and gamma-gamma coincidence.
- Comparison with previous results for the levels 4^+, 6^+, 8^+, 10^+ of the yrast band :

→ New results for the 4^+ and 6^+ excited states.

→ Measurements in γγ gives shorter but compatible lifetime for the 4^+.

→ Lifetime of the 8^+ and the 10^+ states agree with the adopted values.

PRELIMINARY

Jπ	Energy [keV]	τ [ps] adopted*	τ [ps] single γ	τ [ps] coincid γγ
2+	151.8	1800 (400)	/	/
4+	326.5	/	46 (1)	**42 (4)**
6+	486.5	/	5.5 (3)	**6 (1)**
8+	630.1	1.39 (21)	1.2 (2)	**2.5 (10)**
10+	756.6	0.53 (10)	**1.3 (5)**	/

* EVALUATED NNDC, https://www.nndc.bnl.gov/nudat3/

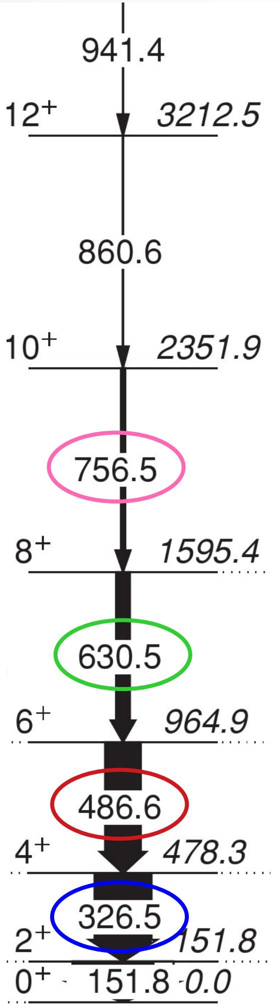

Lifetime measurements in 104Zr

- Preliminary results: lifetime in gamma single.
- Limited amount of statistics (especially at higher energy)
- Measurements possible only in γ single.
- New results for the 4+ and the 6+ excited states.

J^π	Energy [keV]	τ [ps] adopted*	τ [ps] single γ	τ [ps] coincid γγ
2+	139.9	2000 (300)	/	/
4+	312.3	/	**43 (5)**	/
6+	473.7	/	**4 (2)**	/

PRELIMINARY

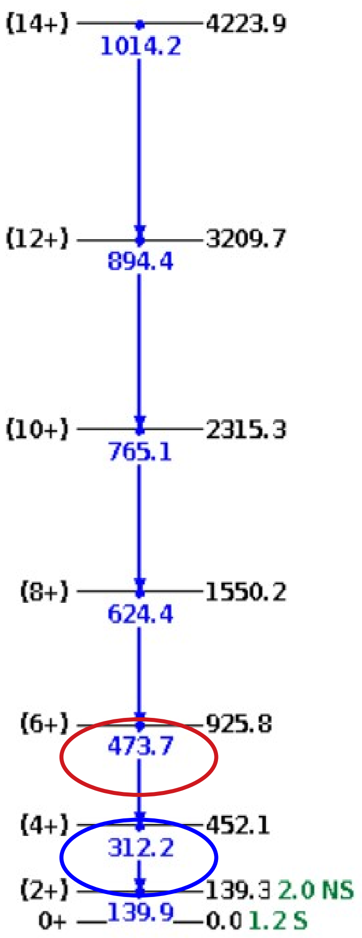

* EVALUATED NNDC, https://www.nndc.bnl.gov/nudat3/

Lifetime measurements in 98Zr

- Preliminary results: lifetime in gamma single and gamma-gamma coincidence.
- Complex level scheme.
- Comparison with previous results.

→ The lifetime of the 2+ and the 4+ are difficult to estimate in γ single because of feedings.

→ The 6^+ and 8^+ lifetimes are in agreement with the adopted values.

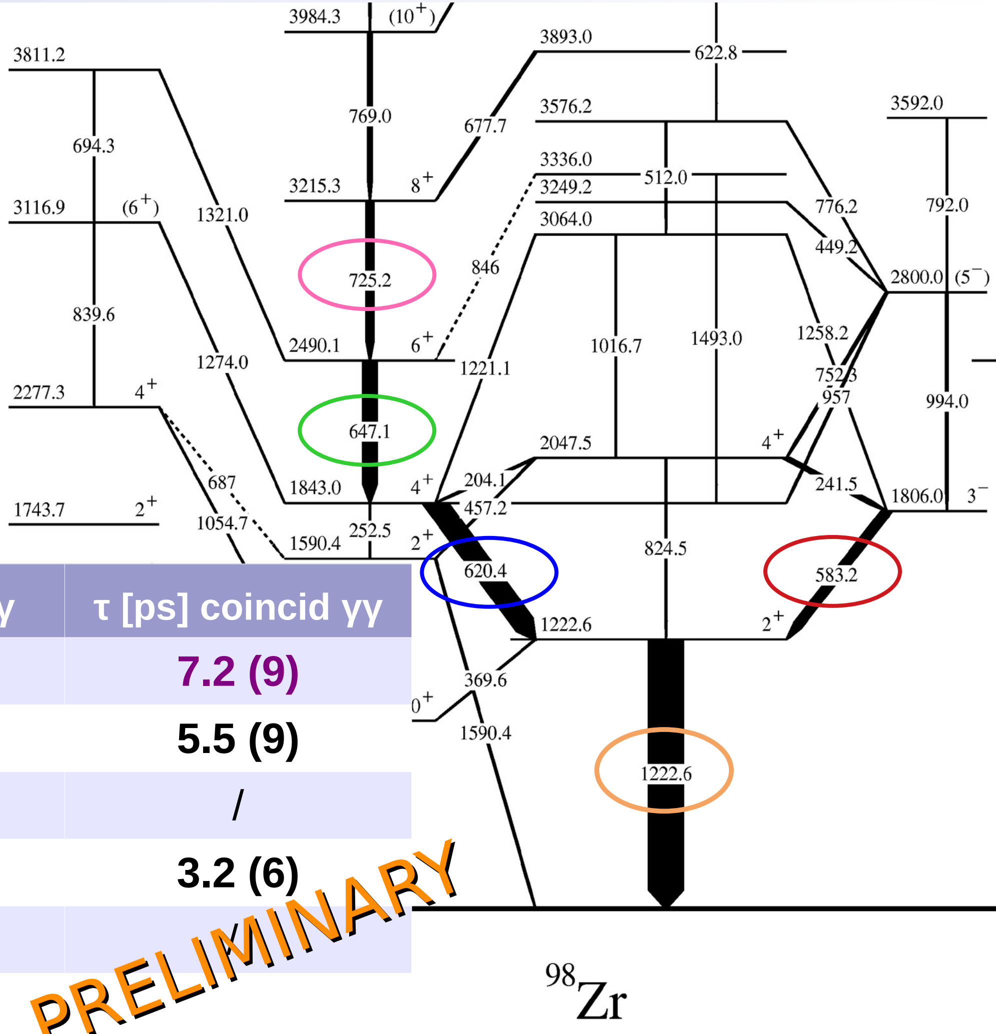

Jπ	Energy [keV]	τ [ps] adopted*	τ [ps] single γ	τ [ps] coincid γγ
2+	1222.9	3.79 (79)	…	**7.2 (9)**
4+	620.5	7.5 (14)	/	**5.5 (9)**
3-	583.3	/	**13 (4)**	/
6+	647.6	2.60 (89)	2.8 (3)	**3.2 (6)**
8+	725.4	2.81 (68)	**2.0 (3)**	/

PRELIMINARY

* EVALUATED NNDC, https://www.nndc.bnl.gov/nudat3/

Comparison with theoretical predictions

- Interacting Boson Model with Configuration Mixing (IBM-CM) N. Gavrielov et al.,PRC 105, 014305 (2022).
- Monte-Carlo Shell Model (MCSM) T. Togashi et al, PRL 117, 172502 (2016).
- BMF within the Symmetry Conserving Configuration Mixing method (HFB-SCCM) T. Rodriguez. (L.M. Robledo, T.R. Rodríguez, and R.R. Rodríguez-Guzmán, Nuclear and Particle Physics 46.1, 013001 (2018).)

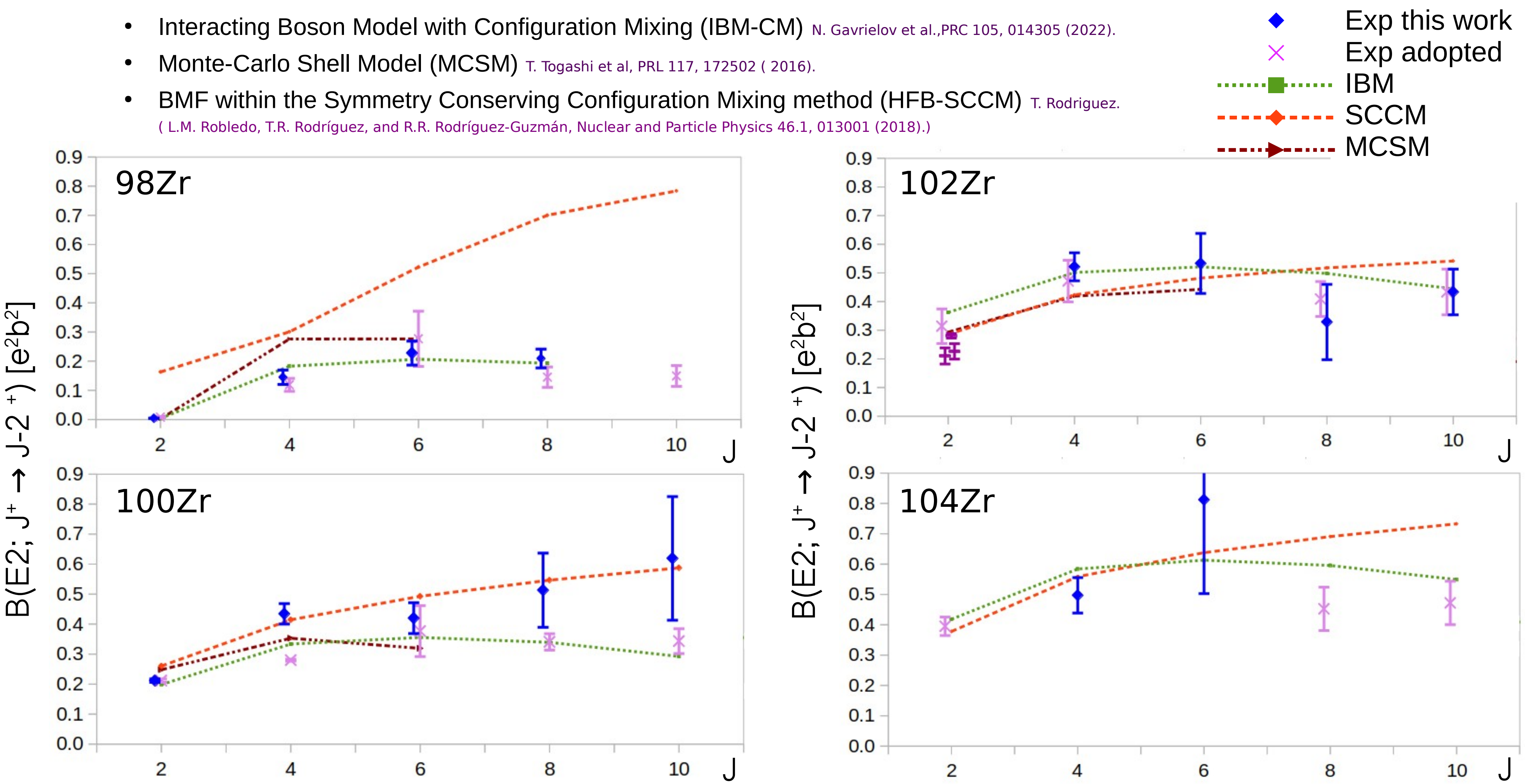

 

Thanks for listening

G. Pasqualato[1], A. Görgen[2], J.S. Heines[2], J. Ljungvall[1], V. Modamio[2], L.G.. Pedersen[2], and W. Korten[3]

[1] *IJCLab, IN2P3/CNRS, Université Paris-Saclay, Orsay, France.*
[2] *Department of Physics, University of Oslo, Norway. and*
[3] *CEA Paris-Saclay, DRF/IRFU/DPhN, Gif-sur-Yvette, France.*

Shape-phase transition in Zr isotopes

Results from recent MCSM calculations: T. Togashi, Y. Tsunoda, T. Otsuka and N. Shimizu, Phys. Rev. Lett. 117, 172502 (2016).

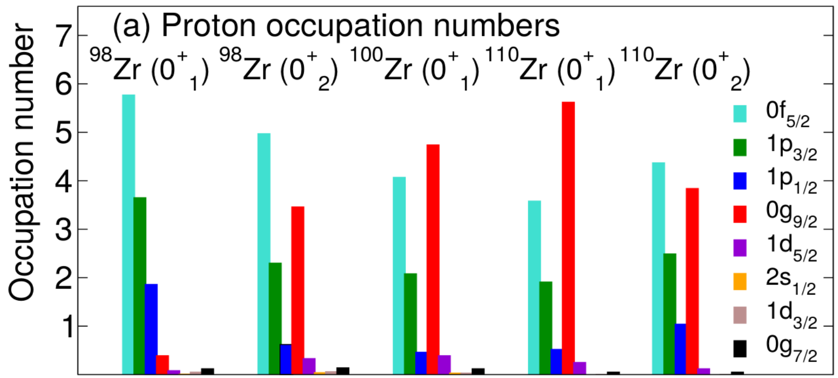

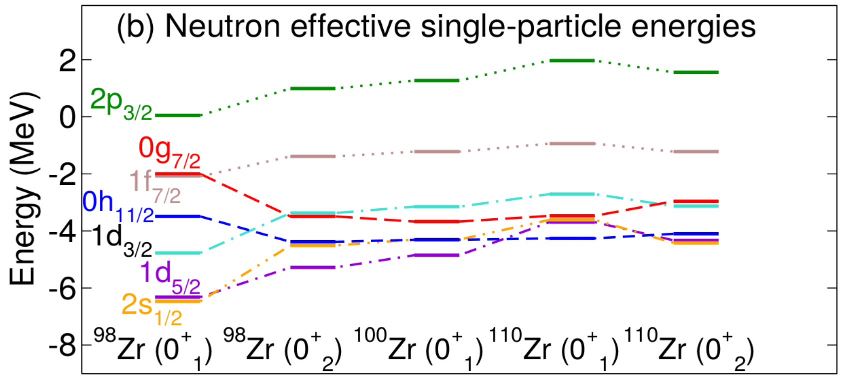

T-plots for $0_{1,2}^+$ states of ^{98,100,110}Zr isotopes to analyze the intrinsic shape of SM eigenstates:

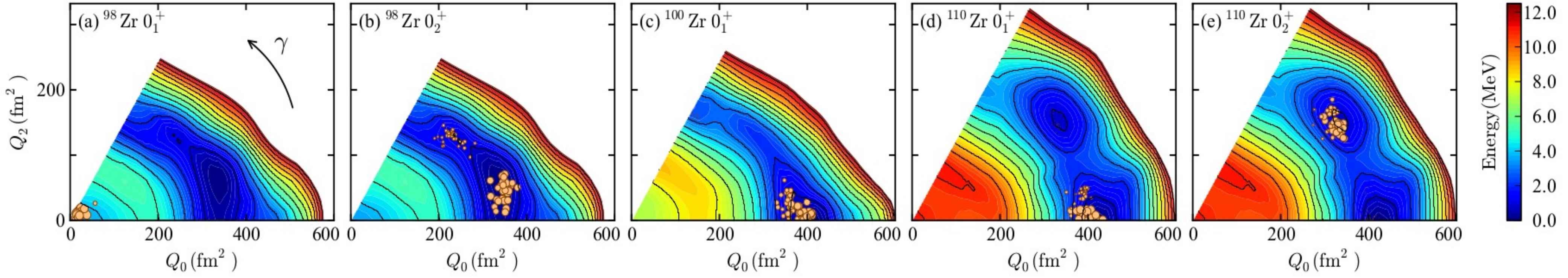

• Production and identification of fission fragments with VAMOS

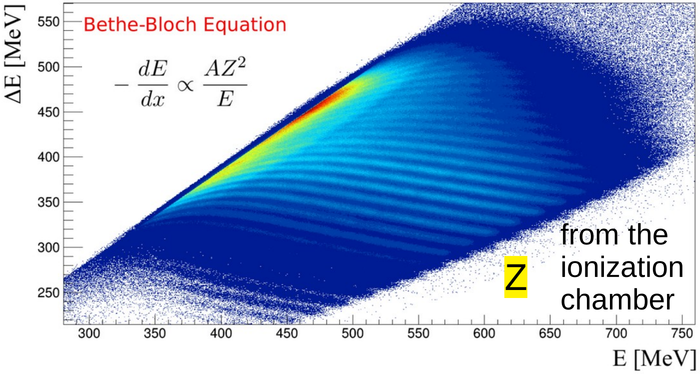

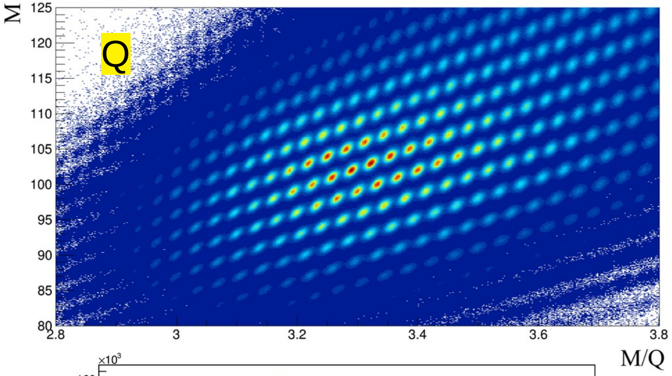

v from the reconstructed trajectory + ToF

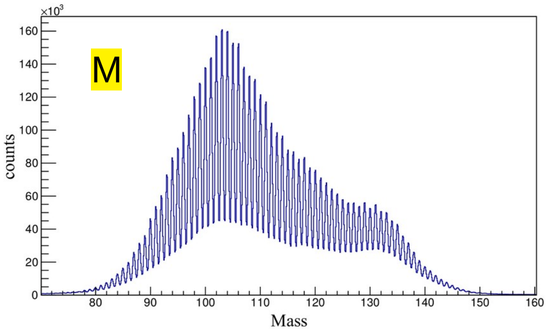

$$B\rho = \gamma \cdot \frac{M}{Q} v$$

$$M_{\text{low res.}} = \frac{E}{(\gamma - 1)c^2}$$ + M/Q → Q

M/Q + Q → M

VAMOS large acceptance magnetic spectrometer

fragment identification based on atomic number Z, mass M and charge Q

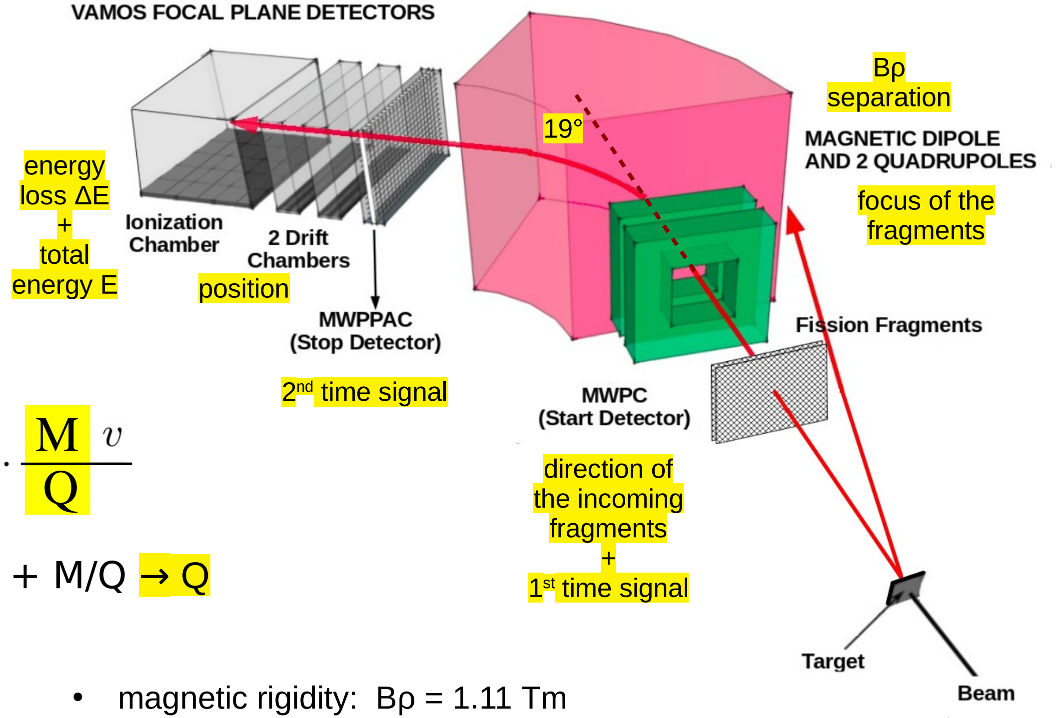

- magnetic rigidity: Bρ = 1.11 Tm
- acceptance = ±10%
- VAMOS position = 19°
- (scattered beam 2° on ^{9}Be, 6° on Mg)

- Production and identification of fission fragments with VAMOS

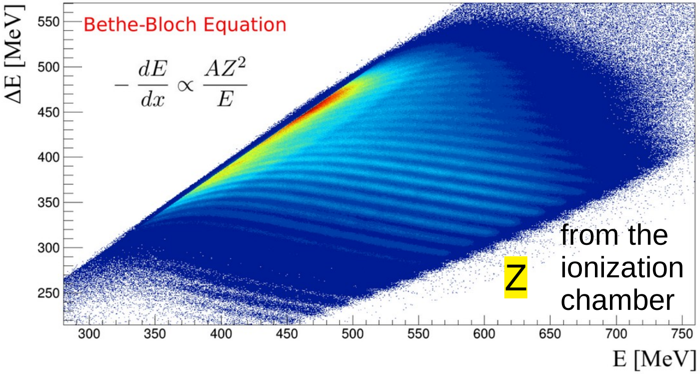

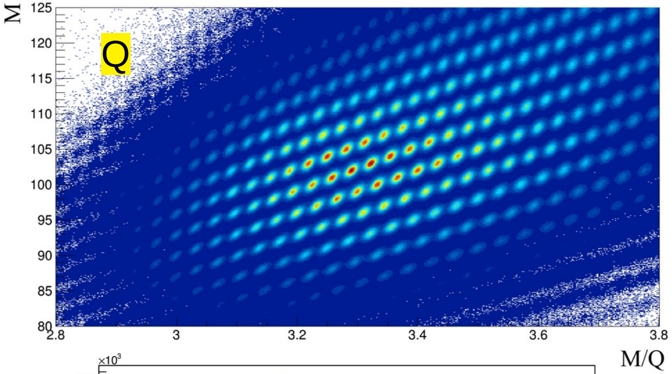

v from the reconstructed trajectory + ToF

$$B\rho = \gamma \cdot \frac{M}{Q} v$$

$$M_{\text{low res.}} = \frac{E}{(\gamma - 1)c^2}$$ + M/Q → Q

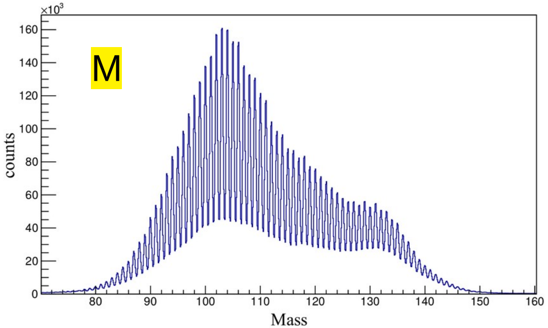

M/Q + Q → M

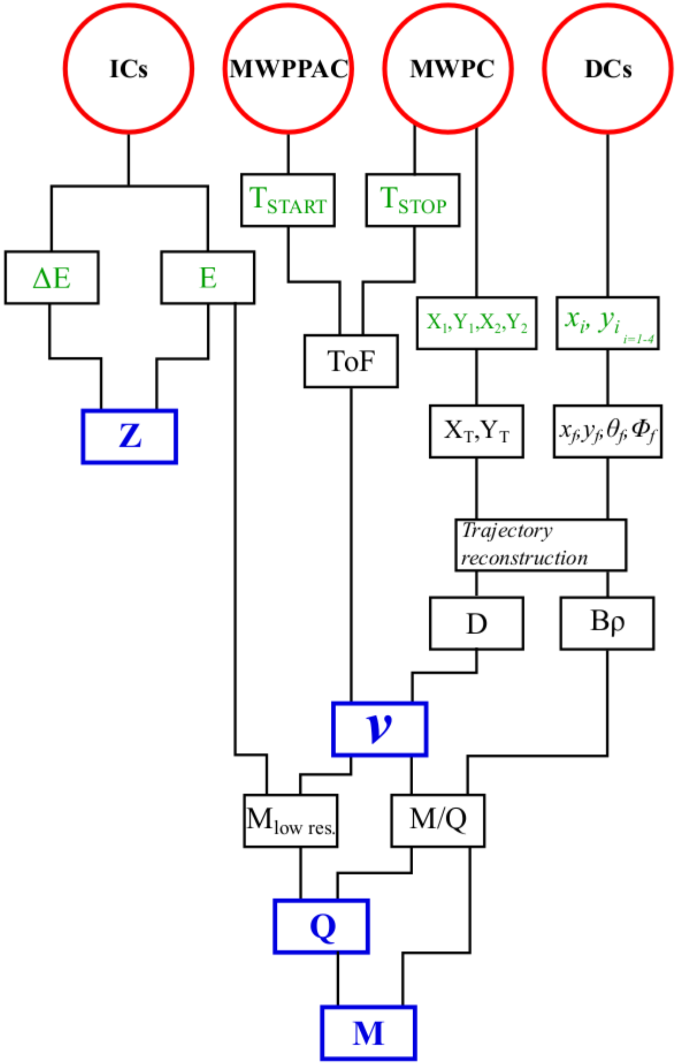

LIFETIME MEASUREMENTS

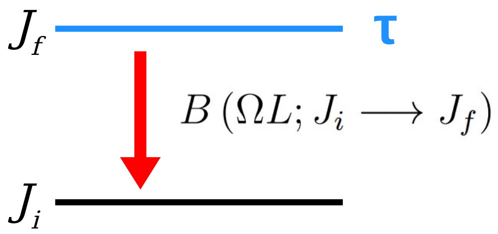

- The lifetime of a nuclear state can range from 10^{-20} seconds to many years . . .
- Different techniques have been implemented

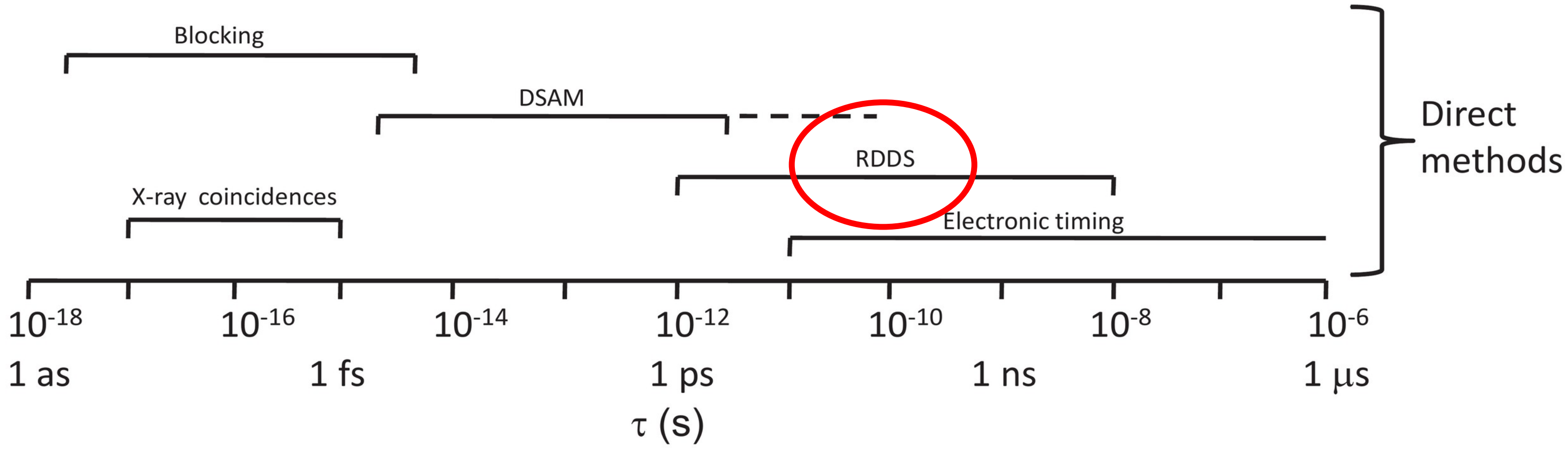

RDDS : Recoil Distance Doppler Shift technique

Feeding for the 4^+ state in ^{100}Zr

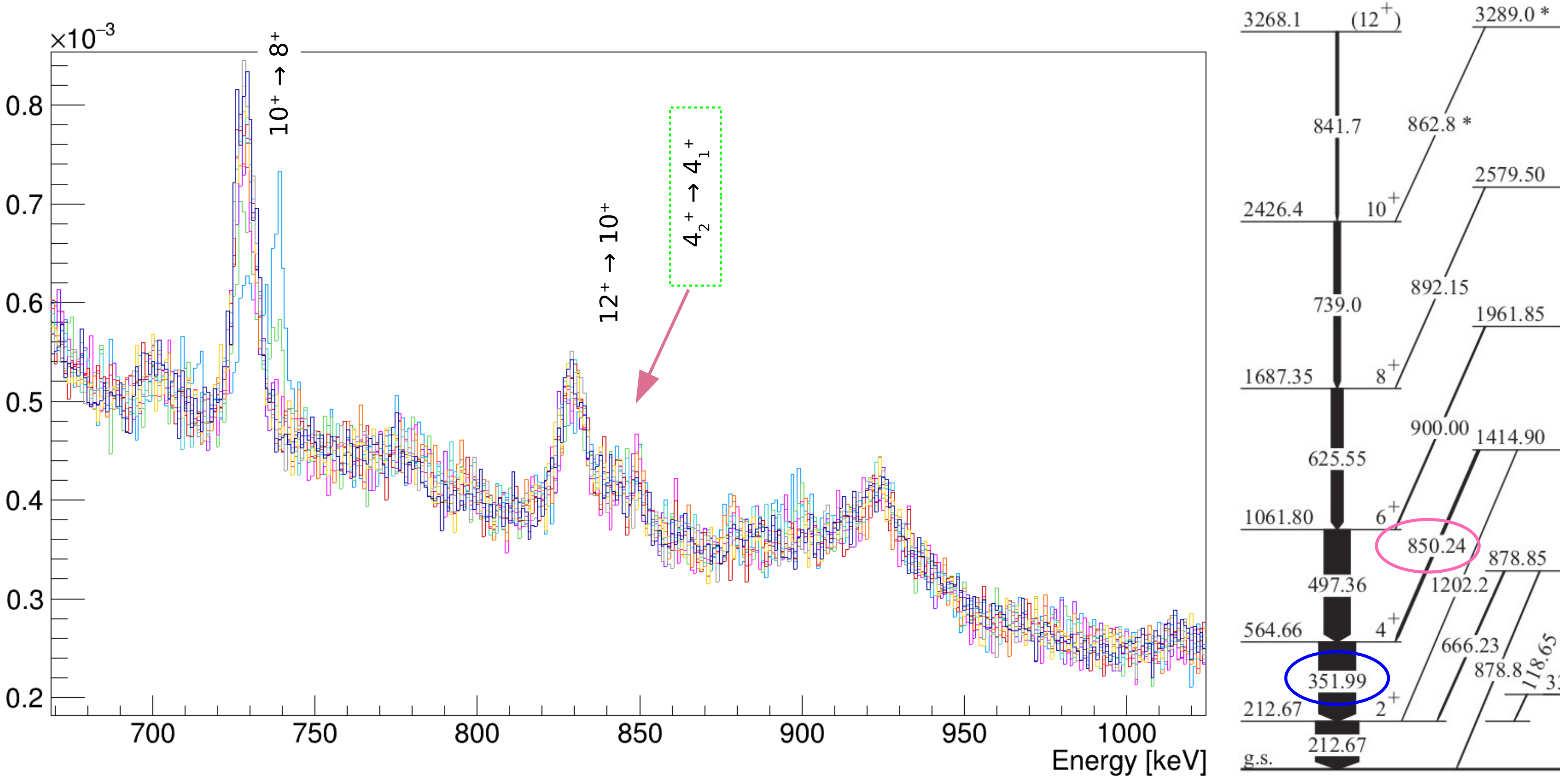

Example of an odd-even system: ^{101}Nb in single γ

Good statistics: many gamma-rays transitions can be resolved in the stooped and shifted component

→ The **complexity of the level scheme** make the DDCM analysis in single γ impossible for this nucleus.

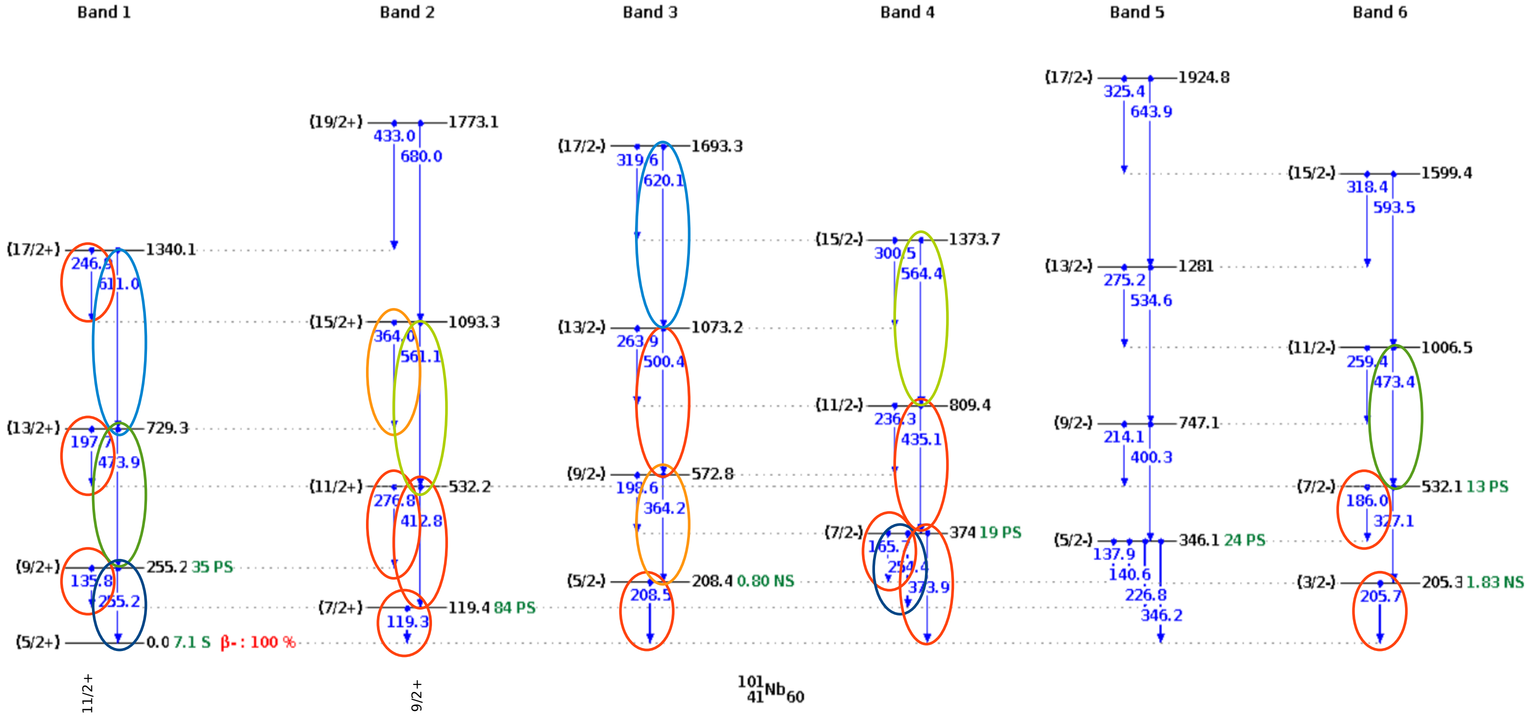

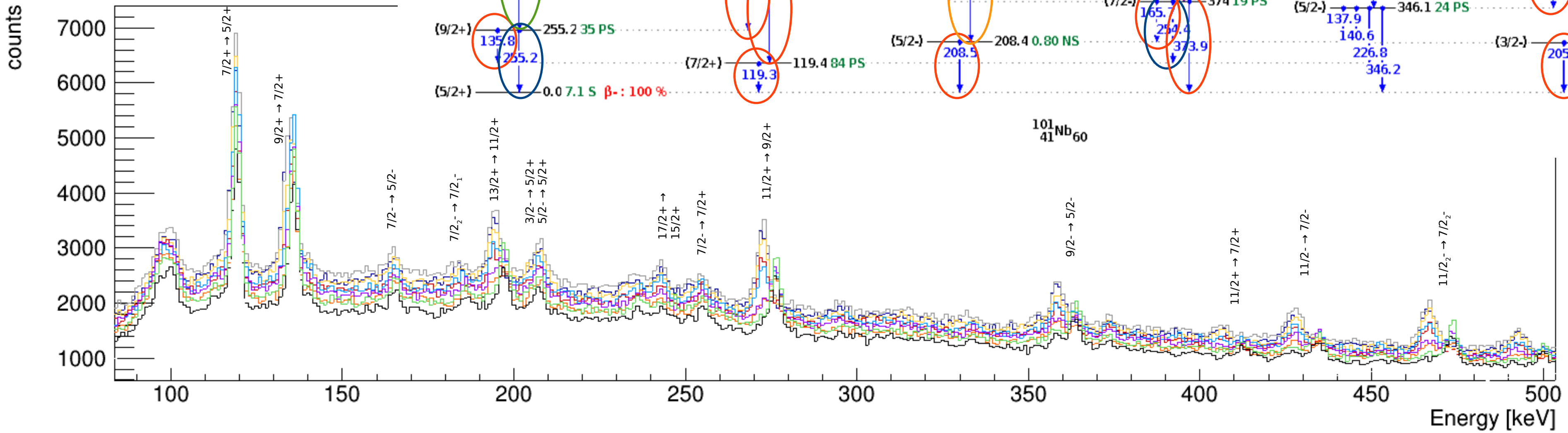

^{98}Zr					
J^π	$\tau_{lit.}$ [ps]	$\tau_{\gamma\gamma}$ [ps]	τ_γ [ps]	E_γ [keV]	$B(E2\downarrow)$ [e^2b^2]
2_1^+	3.79(79) [23], 10(2) [43], ≤6.0 [40], ≥0.68 [41]	7.2(10)		1222.9	0.0041(6)
4_1^+	7.5(14) [23], 13(5) [43], ≤15.0 [40], 29(7) [42]	5.51(94)		620.5(2)	0.145(25)
6_1^+	2.63(89) [23], ≤14 [42]	3.16(57)	2.82(31)	647.58(3)	0.228(41)
8_1^+	2.82(68) [47]		1.95(30)	725.4(1)	0.209(32)
10_1^+	2.05(48) [47]			768.4(1)	

^{100}Zr					
J^π	$\tau_{lit.}$ [ps]	$\tau_{\gamma\gamma}$ [ps]	τ_γ [ps]	E_γ [keV]	$B(E2\downarrow)$ [e^2b^2]
2_1^+	1020(40) [48] 928(75) [45] 840(20) [40]			212.61(4)	
4_1^+	53.4(5) [45] 37(4) [40]	34.4(27)	36.9(6)	351.97(1)	0.510(40)
6_1^+	7.0(16) [45] 12(5) [40]	6.37(78)	6.11(33)	497.36(5)	0.540(65)
8_1^+	2.55(30) [47, 48] 2.49(25) [45]	1.66(40)	1.32(19)	625.55(5)	0.500(120)
10_1^+	1.08(12) [47, 48]		0.72(15)	739.0(1)	0.600(200)

^{102}Zr					
J^π	$\tau_{lit.}$ [ps]	$\tau_{\gamma\gamma}$ [ps]	τ_γ [ps]	E_γ [keV]	$B(E2\downarrow)$ [e^2b^2]
2_1^+	2600(500) [49] 3610(430) [50] 2914(87) [40]			151.8	
4_1^+	46.0(7.1) [40]	41.6(39)	45.9(13)	326.5(2)	0.510(50)
6_1^+	⩽12 [40]	5.6(11)	5.52(33)	486.5(2)	0.540(100)
8_1^+	2.01(30) [47, 48]	2.5(10)	1.18(21)	630.1(5)	0.330(130)
10_1^+	0.77(12) [47, 48]		1.27(52)	756.6(5)	0.260(100)

^{104}Zr					
J^π	$\tau_{lit.}$ [ps]	$\tau_{\gamma\gamma}$ [ps]	τ_γ [ps]	E_γ [keV]	$B(E2\downarrow)$ [e^2b^2]
2_1^+	2900(250) [51]			139.3	
4_1^+			43.4(51)	312.2(3)	0.450(40)
6_1^+			4.2(16)	473.7(3)	0.850(400)
8_1^+	1.91(29) [47, 48]			624.4(3)	
10_1^+	0.67(10) [47, 48]			765.1(3)	

Lifetime results from this work. Comparison with all existent measurements.

G. Pasqualato et al., PRC to be submitted (2022)

[23] P. Singh et al., Phys. Rev. Lett. 121 (19), 192501 (2018).
[40] S. Ansari *et al.*, Phys. Rev. C 96, 054323 (2017).
[41] W. Witt *et al.*, Phys. Rev. C 98, 041302(R) (2018)
[42] L. Bettermann, J.-M. Régis, T. Materna, J. Jolie, U. Kster, K. Moschner and D. Radeck, Phys. Rev. C 82, 044310 (2010).
[43] V. Karayonchev et al., PRC 102, 064314 (2020).
[44] H. Ohm, M. Liang, G. Molnár and K. Sistemich, Z. Physik A-Atomic Nuclei 334, 519 (1989).
[45] A.G. Smith *et al.*, Journal of Physics G: Nucl. Part. Phys. 28, 2307 (2002).
[46] P.J. Nolan and J.F. Sharpey-Schafer, Rep. Prog. Phys. 42 1 (1979).
[47] A.G. Smith, J.L. Durell, W.R. Phillips, W. Urban, P. Sarriguren and I. Ahmad, Phys. Rev. C 86, 014321 (2012).
[48] A.G. Smith *et al.*, Phys. Rev. Lett. 77, 1711 (1996).
[49] S. Raman, C.W. Nestor JR. and P. Tikkanen, Atomic Data and Nuclear Data Tables 78, 1-128 (2001).
[50] F. Browne *et al.*, Acta Phys. Pol. B 46, 721 (2015).